APPLICATION OF CONTINUUM MECHANICS TO COMPACTION IN TILLABLE SOILS

by

Glen Edwin Vanden Berg

AN ABSTRACT

Submitted to the School for Advanced Graduate Studies of

Michigan State University of Agriculture and

Applied Science in partial fulfillment of

the requirements for the degree of

DOCTOR OF PHILOSOPHY

Department of Agricultural Engineering

Year 1958

ABSTRACT

To study the compaction problem, the resulting change in soil compaction at each point caused by an applied load needs to be determined. This can be accomplished if a suitable mathematical model of soil is available, such as the Theory of Elasticity is for metals. Unfortunately, such a model for soils does not exist at this time.

The development of a suitable soil mechanics requires specifying the forces acting on a small volume element of the soil and specifying the deformation of the volume element resulting from the applied forces. The mechanics of the continuum presents a rigorous mathematical method for specifying both the forces and the deformation: the first results in a stress tensor and the second in a strain tensor. The desired mechanics would result if the relationship between the two tensors could be determined. Because of the complexity of the soil, the determination of the above relationship does not seem feasible at the present time.

A simplification of the problem is possible by ignoring the shearing deformations and rigid body rotation. The volume change or volume strain can be expressed as a change in bulk density of the volume element independent of the shearing and rotation. A stress-compaction relationship for soils can thus be developed by relating the stress tensor to bulk density. Theoretical considerations suggest that the mean normal stress, an invariant of the stress tensor, controls volume change. An experiment was designed to test this hypothesis by

measuring the stress tensor and the bulk density 'at the same point' in the soil while the soil was subjected to static loads of various magnitudes. A laboratory method for testing the hypothesis using triaxial apparatus was also developed which permits laboratory control of the soil and applied loads.

Because of its suitable facilities, the National Tillage Machinery Laboratory, Auburn, Alabama, was chosen for the testing program. Three different soil types -- sandy loam, silty clay loam, clay -- were tested. Limited time at the Laboratory permitted only preliminary studies with the triaxial apparatus.

The time-consuming calculations of evaluating invariants of the stress tensor besides the mean normal stress were reduced by using MISTIC, an electronic digital computer at Michigan State University. Because of large variations in the data and small difference in stress states obtained, a simple, rapid, graphical method of estimating the standard error was used. The data indicated that of four invariants of the stress tensor investigated, the mean normal stress was the best invariant to relate to bulk density. However, it could not be concluded that other invariants of the stress tensor were not related to bulk density. This supports the hypothesis that mean normal stress is related to bulk density, but does not prove it.

Other conclusions from the data were as follows: a) triaxial apparatus can be used to study stress-bulk density relationships in

tillable soils; triaxial data in the sandy loam soil agreed with field data of the same soil: the agreement verifies both methods of testing; b) the distribution of mean normal stress appears to be independent of soil type and determined only by the geometry of loading; c) the mean normal stress-bulk density relationship appears to be exponential for all soils studied; d) stress distributions predicted by the Theory of Elasticity did not agree with measured distributions.

APPLICATION OF CONTINUUM MECHANICS TO COMPACTION IN TILLABLE SOILS

by

Glen Edwin Vanden Berg

A THESIS

Submitted to the School for Advanced Graduate Studies of Michigan State University of Agriculture and Applied Science in partial fulfillment of the requirements for the degree of

DOCTOR OF PHILOSOPHY

Department of Agricultural Engineering

Year 1958

ACKNOWLEDGEMENTS

The author wishes to express his sincere appreciation to the following:

Doctor A. W. Farrall, for providing an assistantship and the necessary funds to carry out the investigations;

The guidance committee composed of Doctor W. F. Buchele, (chairman), Doctor A. E. Erickson, Doctor L. E. Malvern, Doctor D. J. Montgomery and Doctor E. A. Nordhaus, for their encouragement and assistance. The author is particularly indebted to Doctor Buchele for his continuous guidance throughout the program and to Doctor Malvern for his many hours in consultation;

Doctor W. M. Carleton and Professor H. F. McColly, for their leadership during the organization of the program of study;

Doctor A. W. Cooper and the staff of the National Tillage Machinery Laboratory, Auburn, Alabama, for their vital contribution to the investigations;

Phyllis, my wife, for her faith and encouragement, and assistance in preparation of the manuscript.

VITA

Glen Edwin Vanden Berg

Candidate for the degree of

Doctor of Philosophy

Final examination:

June 24, 1958; 1:15-3:15
Room 218, Agricultural Engineering Department

Dissertation:

Application of Continuum Mechanics to Compaction in Tillable Soils

Outline of Studies:

Major Subject	Agricultural Engineering
Minor Subjects	Mathematics
	Applied Mechanics

Biographical Items:

Born August 12, 1930, Volga, South Dakota

Undergraduate studies at South Dakota State College, Brookings, 1948-1952 (B.S. in Agricultural Engineering)

Graduate studies at Michigan State University, East Lansing, 1955-1956 (M.S. in Agricultural Engineering)

Experience:

Intermediate speed radio operator (International Morse Code) and Troop Information and Education NCO in U.S. Army, 1952-1954; Graduate Research Assistant, Mich. State Univ.,1955-1958

Member:

American Society of Agricultural Engineers; Phi Kappa Phi; Pi Mu Epsilon; Sigma Pi Sigma; Society of the Sigma Xi; Alpha Zeta

TABLE OF CONTENTS

LIST OF FIGURES

INTRODUCTION

The effect of the physical properties of soil upon plant growth is receiving increased attention. Fertilizers, placement of fertilizers and similar cultural practices have increased production. A plateau, however, has been reached wherein higher rates of fertilizer application, for example, do not materially increase production. The reason for this is apparently that the physical state of the soil has become the major limiting factor in crop yields. The state of consolidation of soil, popularly known as soil compaction, is one of the soil's physical properties. It has been shown that mechanical impedance to roots, infiltration rate, percolation rate, oxygen availability and nitrogen availability are all influenced to some degree by the state of compaction of the soil. (Baver, 1956; Gill, 1954; Wadleigh, 1957; Wiersma and Mortland, 1953.)

In some areas of California, Hawaii and portions of the southern United States as well as other random regions, the degree of compaction has reached a level that has seriously reduced yields and in some cases removed land from cultivation. (Edminster, 1956.) Since these areas have been removed from production, it behooves all civilizations to study the compaction problem before other areas are removed from production. Even further, the reduced yields from incorrect compaction levels during tillage operations, planting for example, cannot even be estimated. In certain cases additional compaction may be desired.

At the present time, there is no known method for producing a desired state of compaction during tillage operations other than trial and error. The state of compaction resulting from a single operation by any given tillage tool cannot be predicted except through experienced judgment. In this respect, tillage has not advanced far from the days when seeds were planted in a hole punched in the soil with a pointed stick. As continued investigations reveal new knowledge concerning the desired degree of compaction for a given crop, the need for a method to produce such a degree becomes increasingly important.

The largest measured forces applied to the soil were under the rear wheel of a farm tractor. (Vanden Berg, et.al., 1957.) While such mechanical forces are not the only causes of soil compaction, they are the major cause today. Heavier tractors and implements coupled with increased numbers of trips over the soil (resulting from new cultural practices such as fertilizing and spraying) apply repeated loads to the soil. To understand the effect of these loads on the soil, the amount of compaction change at every point in the soil resulting from an applied load must be determined. A solution to the problem may be secured by changing the manner in which the load is applied and observing the corresponding compaction changes. In this way the best method for applying the load can be determined; or at least the knowledge to predict the amount of compaction change can be obtained.

To carry out the study indicated above by measuring the compaction change under various loads in various soils would seemingly require a prohibitive amount of time. It is imperative, therefore, that a more organized approach be attempted. If a suitable mechanical model for soils, such as the Theory of Elasticity provides for metals, could be found it would be possible to calculate the desired volume change. At the present time, no suitable soil mechanics model is available.

This thesis will present a method whereby a soil mechanics model based upon the concept of continuum mechanics can be developed. The representation of forces acting on and the representation of compaction change in a volume element of soil will be discussed. An hypothesis concerning the relationship between the forces acting on the volume element and the compaction change in the element will be proposed. The analysis of data taken to test the hypothesis is presented and analyzed.

REVIEW OF LITERATURE

'An agricultural soil in a good state of tilth is a poor road surface and in most cases it is damaged, at least temporarily, by the passage of a transport wheel.' (McKibben and Green, 1940.) This load sets up a stress distribution throughout the soil and according to McKibben and Green, results in subsequent damage to the soil. Today this mechanical consolidation of the soil has been named soil compaction. In speaking of the stress distribution above, Hogentogler (1937) stated, 'The volume of compressed soil included between the points of zero pressure and the bearing block (load) is known as the pressure bulb...The supporting power of the bulb is developed by the resistance to deformation offered by the cohesion and internal friction of the soil.' Obviously, if this stress distribution and the relationship between stress and the resistance offered by the supporting bulb described above were known, the change in compaction resulting from loads could be calculated.

There have been several attempts to evaluate stress distribution in the soil. In 1885 Boussinesq developed formulae that give stresses in an isotropic homogeneous medium that obeys Hooke's law when subjected to a point load. In 1934, O. K. Froehlick introduced a concentration factor into the formulae which permits some generalization of the stress distribution. Soehne (1953) estimated the contact area under various tractor tires and divided the area into 25 smaller areas.

Considering the load acting on each little area as a point load located at the centroid of the area and using Froelick's formulae he then summed all the contributions of each area at several points below the load and arrived at a stress distribution.

An attempt to determine the stress distribution under circular loads was developed by Love and applied by the Corps of Engineers (1953,) This approach was somewhat better than the one presented by Soehne since it was not restricted to point loads. Love's formulae also apply only to an isotropic homogeneous medium which obeys Hooke's law. There is considerable evidence that soil does not obey Hooke's law. The modulus of elasticity changes not only with soil types and conditions but also as a load is applied. (Corps of Engineers, 1954.) Furthermore the elastic recovery after compaction is very small, indicating little elastic behavior. (Gill and Reaves, 1956.) Since soils exhibit little elastic behavior, the stress distributions based on elasticity should be questioned.

Several attempts have been made to check the theories giving stress distributions and some have met with reasonable success as reported by the Corps of Engineers (1954.) Their tests were most successful on sand. Plummer and Dore (1940) had the following to say about other earlier tests: 'Unfortunately, almost all actual tests have been conducted on soils consisting of dry, granular masses such as sands. There is some reason to believe that some soils approach, in their supporting action, that of a very viscous material such as asphalt...We cannot at present predict with any great accuracy the magnitude of stress at a given point in such soils.' From the above it seems quite clear that at the present time there is no way to accurately determine stress distributions in the soil.

Attempts have been made to go directly from the applied load to soil compaction but many problems have been encountered. (Gill and Reaves, 1956.) This reference stated that 'many difficulties were encountered when attempts were made to relate soil compaction to the compactive pressures by tires to the soil. Measurement of the contact pressure is difficult and not yet satisfactorily measured; yet, given this pressure in the soil, other complicating factors remain.' Thus the more basic approach of determining the stress distribution and the exact relationship between stress and compaction should lead to a better solution of the problem.

Soehne (1953) assumed a relationship between stress and compaction and proceeded to measure the relationship on undisturbed soils. He assumed that the maximum normal stress acting on the soil element related best to soil compaction. He then made the measurements by applying a surface load to the soil in a confined container. In so doing, he ignored the side stresses acting on the soil. It seems that these side stresses should be taken into account as well as the maximum normal stress.

The application of strain gages in designing cells led to the first real progress in accurately measuring soil stresses. The use of several types of these cells is reported in several sources. (Cooper, et. al., 1957; Corps of Engineers, 1954; Peattie and Sparrow, 1954; Willits, 1956.) The performances of the cells presented by Cooper makes it preferable to the other types. The cells of the Corps of Engineers, while probably as accurate as those developed by Cooper, are more expensive and perhaps larger than desirable for application to agricultural soils. There is little doubt from the work of Cooper and the Corps of Engineers that the cells measure soil stress accurately when properly used.

THEORY - MECHANICS OF THE CONTINUUM

As mentioned before, if a good mathematical description of the soil existed, the compaction change in the soil for any combination of applied loads could be calculated. Such a description of the soil does not exist today. To develop the needed soil mechanics, the forces acting on a volume element of soil must be related to the deformation of the volume element. The mechanics of a continuous medium provides a method for specifying the forces acting on a volume element of the soil and a method for specifying the deformation of the volume element resulting from the applied forces. As is known, the former results in a stress tensor and the latter in a strain tensor. A relationship between the two tensors provides the desired mechanics mentioned above.

In dealing with soil compaction, it is possible to simplify the strain tensor by ignoring the shearing strains and rigid body rotations. The change in compaction is merely the change in the volume of the element and is independent of any shearing or rotating that may take place during straining. The compaction of the volume element can be completely specified by giving its bulk density, i.e. the weight of oven dry soil per unit bulk volume; the bulk volume includes both volume of soil solids and soil pores. The bulk density of each volume element in a body of soil specifies completely the state of compactness of the body of soil. A compaction law can thus be developed by relating the stress tensor to bulk density. In so doing it follows from above that all shearing and rotating deformations will be ignored. If a relationship between the stress tensor and the complete strain tensor could be developed, the exact position of each soil element as well as the volume change of each element could be accurately calculated. Because a complete solution is not of immediate concern, ignoring the shearing and rotating deformations provides a suitable means of simplifying the problem.

To describe the forces acting on a volume element, the concepts of the stress vector and the stress tensor are required. If an imaginary plane is passed through a point in some medium subjected to general forces, the material on one side of the plane exerts a force across the plane on the other side of the material. In Fig. 1, for example, the force exerted across the area ΔA by part (1) of the body on part (2) of the body is represented by the vector $\overrightarrow{\Delta P}$. The stress vector $\vec{T}$ at the point O is then defined as

$$\vec{T} = \lim_{\Delta A \to 0} \frac{\overrightarrow{\Delta P}}{\Delta A} .$$

Existence of the limit requires the medium to be continuous and without holes or gaps. This idealization is applicable only if the theory is applied to samples large in comparison to the gaps or pores which are actually present. In the case of soil this requirement is easily met since the sensing elements used to measure stress require an area much larger than the size of individual soil particles. The cells thus

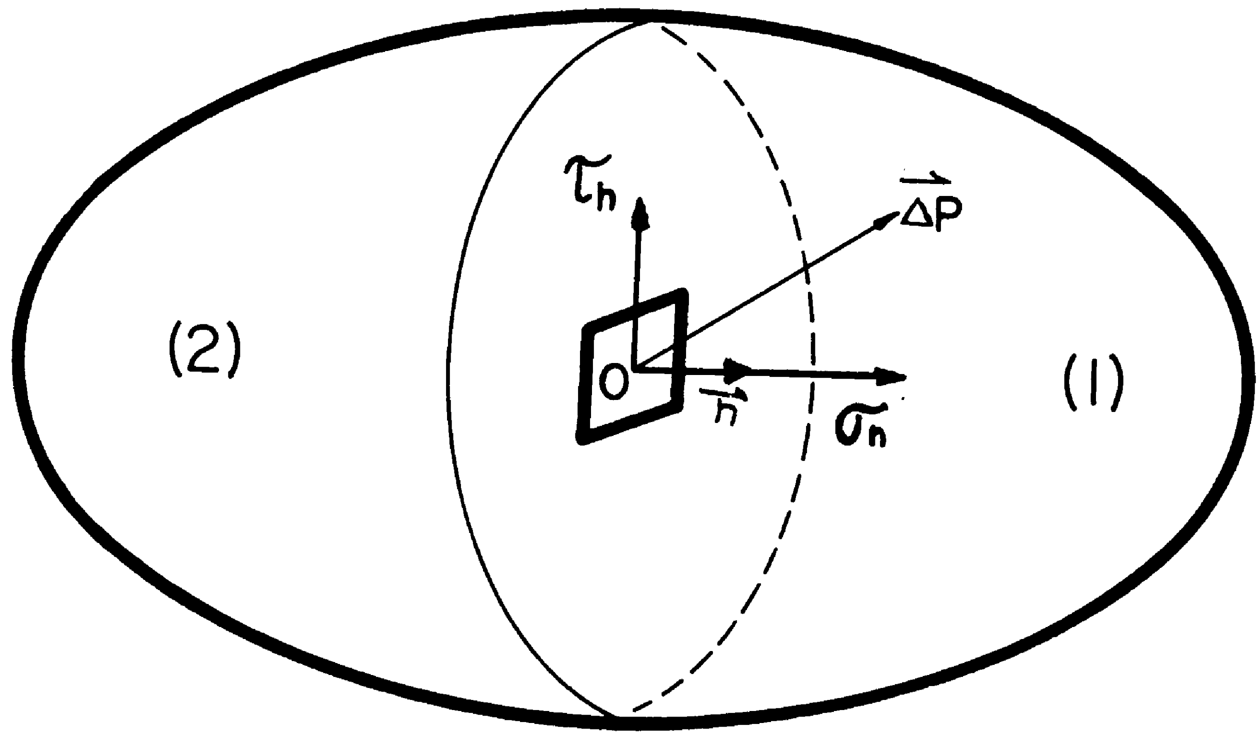

FIG. 1 STRESS VECTOR ON A PLANE

measure the average stress over an area.

In general, the stress vector has two components - one normal to the plane on which it acts and one tangent to the plane. These stresses represent different physical actions on the plane and are distinguished as such in the notation. The first component is the normal stress and is denoted by the Greek letter σ with an appropriate subscript; the latter component is the shearing stress and is denoted by the Greek letter τ , again with appropriate subscript. Thus in Fig. 1 where the plane is identified by the direction of its normal $\vec{n}$ (drawn outward from the body on which the stress acts) the normal stress component is σ_n and the shear component is τ_n.

In general, if a different plane is passed through the same point, a different stress vector will act across it. Hence, the stress vector depends not only on the position of the point in the body but also on the orientation of the plane through the point. An infinite number of orientations may be chosen for a plane through any point; it is necessary to be able to determine the stress vector on all of these planes. It can be shown that the specification of the stress vectors on three mutually perpendicular planes completely determines the stress state at any point. From these three stress vectors, the stress vector on any other plane through the point can be calculated. The procedure for doing this will be presented later.

In Fig. 2, the three reference planes are represented as three faces of a cube perpendicular respectively to the X, Y, and Z axes of conventional cartesian coordinate system. The shear stress components in each of these faces are further resolved into two components each parallel to a coordinate axis; the symbols representing them are given two subscripts. The first subscript identifies the plane on which it acts and the second identifies the direction in which it acts. These nine quantities

$$\begin{pmatrix} \sigma_x & \tau_{xy} & \tau_{xz} \\ \tau_{yx} & \sigma_y & \tau_{yz} \\ \tau_{zx} & \tau_{zy} & \sigma_z \end{pmatrix}$$

are the components of the stress tensor at a point referred to a chosen set of axes. Note that the cube in Fig. 2 is imagined to be infinitesimal so that the stresses on the three front faces act 'at the point O' in the limit as the volume of the element shrinks to zero. From equilibrium conditions it can be shown that $\tau_{xy} = \tau_{yx}$, $\tau_{xz} = \tau_{zx}$ and $\tau_{yz} = \tau_{zy}$. This leaves six independent values to be determined to define the state of stress at a point.

The stress vector on an arbitrary plane can most easily be calculated by using matrix algebra since the stress tensor can be represented as a 3 x 3 matrix. The calculation is accomplished in the following manner:

Suppose a plane is oriented so that its normal lies in the YZ plane and bisects the angle between the positive Y and Z axes. The normal to the plane will have direction cosines O, $\sqrt{2}/2$, $\sqrt{2}/2$,

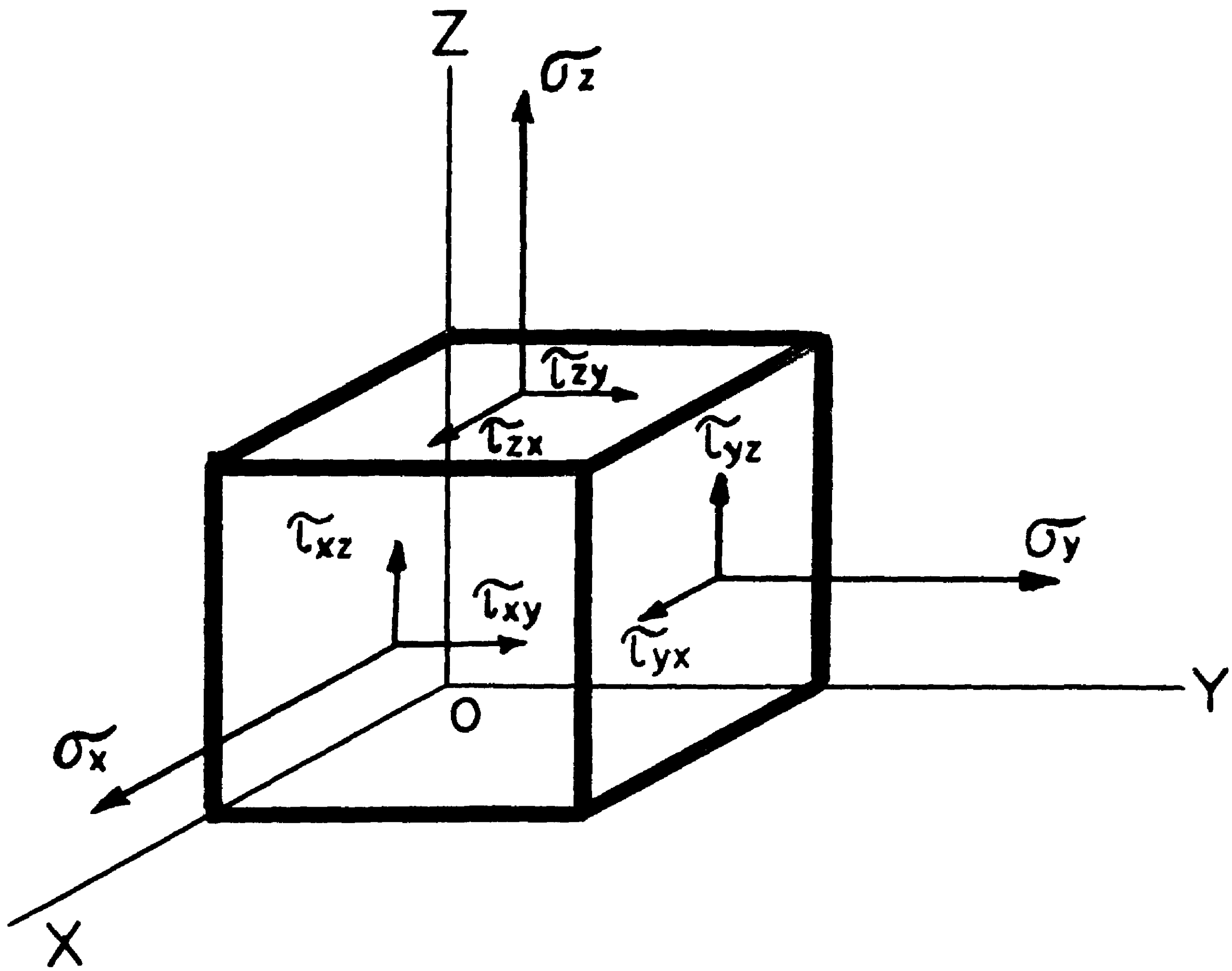

FIG. 2 STRESSES ON A VOLUME ELEMENT

respectively with the X, Y and Z axes. The direction cosines can be written in a row matrix as follows:

$$\begin{pmatrix} 0 & \sqrt{2}/2 & \sqrt{2}/2 \end{pmatrix}.$$

Let us further suppose that the stress state is a special one in which two of the shearing stresses are zero. The stress tensor for this special stress state is given by

$$\begin{pmatrix} \sigma_x & 0 & 0 \\ 0 & \sigma_y & \tau_{yz} \\ 0 & \tau_{yz} & \sigma_z \end{pmatrix}.$$

If $\vec{i}$, $\vec{j}$, and $\vec{k}$ are unit vectors along the positive X, Y, and Z axes respectively, then the components of the stress vector acting on the plane described above are given by the matrix multiplication shown below. Using the usual method of multiplying rows into columns, the stress vector $\vec{T}$ is

$$\vec{T} = \begin{pmatrix} 0 & \sqrt{2}/2 & \sqrt{2}/2 \end{pmatrix} \begin{pmatrix} \sigma_x & 0 & 0 \\ 0 & \sigma_y & \tau_{yz} \\ 0 & \tau_{yz} & \sigma_z \end{pmatrix}$$

$$= 0\,\vec{i} + \left(\sqrt{2}/2\,\sigma_y + \sqrt{2}/2\,\tau_{yz}\right)\vec{j} + \left(\sqrt{2}/2\,\tau_{yz} + \sqrt{2}/2\,\sigma_z\right)\vec{k}.$$

The magnitude of the normal stress acting on the plane can be found by obtaining the scalar product of a unit vector $\vec{n}$ in the direction of the normal to the plane and the stress vector $\vec{T}$ acting on the plane. The unit normal vector $\vec{n}$ is given by

$$\vec{n} = 0\,\vec{i} + \sqrt{2}/2\,\vec{j} + \sqrt{2}/2\,\vec{k}\,.$$

Thus the normal stress, σ_n, on the plane is

$$\sigma_n = \vec{n}\cdot\vec{T} = \left[\sqrt{2}/2\,\vec{j} + 2/2\,\vec{k}\right]\cdot\left[\sqrt{2}/2\left(\sigma_y + \tau_{yz}\right)\vec{j} + \sqrt{2}/2\left(\tau_{yz} + \sigma_z\right)\vec{k}\right]$$

$$\sigma_n = 1/2\left(\sigma_y + \sigma_z\right) + \tau_{yz}\,. \tag{1}$$

The stress tensor has several mathematical properties of interest. It is always possible to rotate the coordinate axes (and with them the imaginary planes bounding the cubical volume element) to such a position that all of the shear stresses will be zero and only normal stresses act on the planes. In this position the axes are called the principal axes or principal directions of the stress tensor at the point. The three normal stress in these directions are the principal stress at the point denoted by σ_1, σ_2, and σ_3 as in Fig. 3. One of these principal stresses is the largest normal stress on any possible plane through the point and another one is the smallest possible normal stress through the point. The principal axes orientations and the principal stress magnitudes are not the same at all points. It is possible, however, to calculate for any one point the magnitude and orientation of the principal stresses when the stress tensor components are known with reference to some system of coordinate axes. The problem is to determine the direction cosines n_x, n_y, n_z so that the stress vector associated with the plane determined by the direction

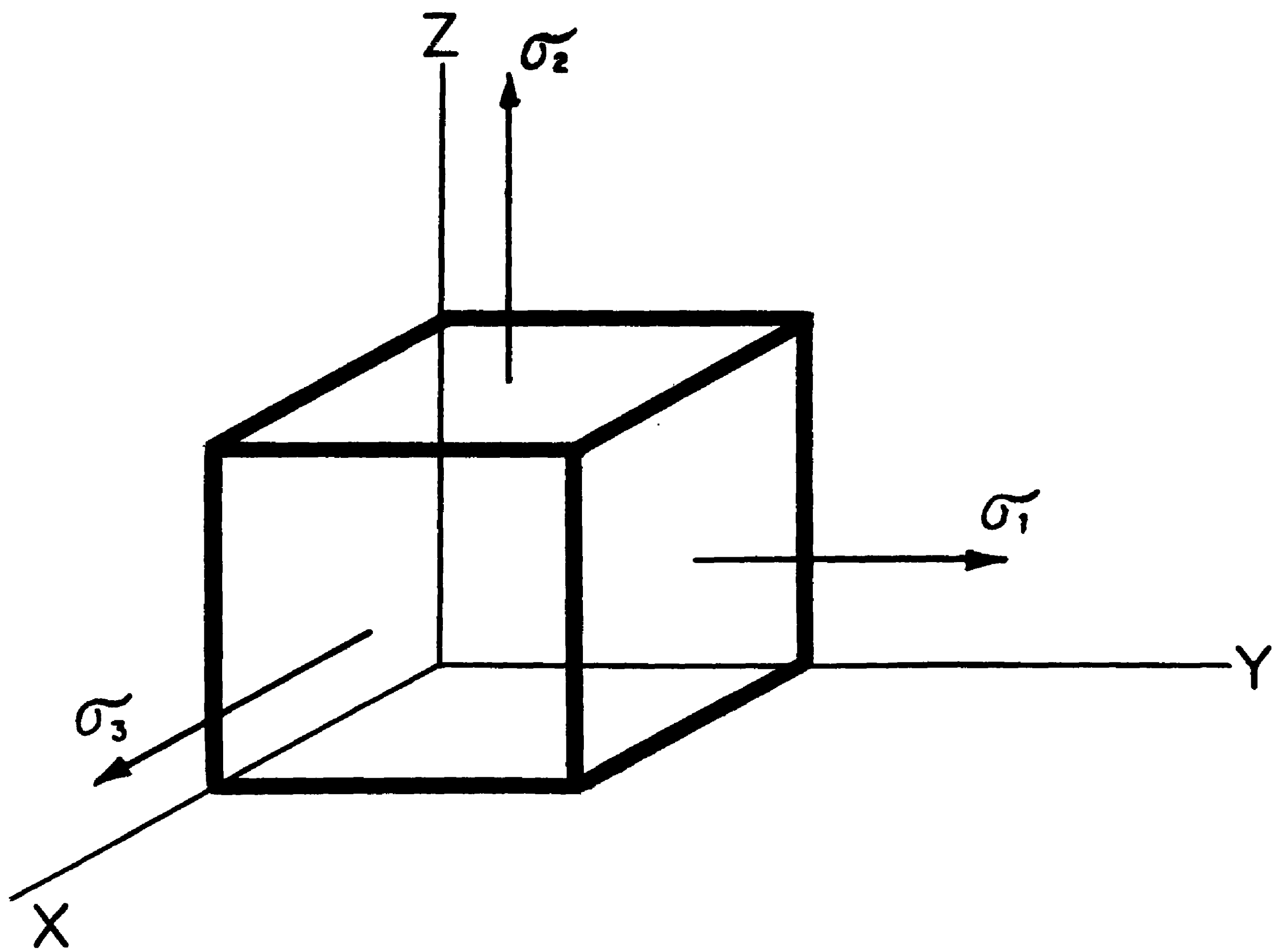

FIG. 3 PRINCIPAL STRESSES ON A VOLUME ELEMENT

cosines is normal to the plane. For example, in the special stress state used above, σ_x must be a principal stress since the plane on which it acts has no shear components. Therefore, the other two principal stresses must lie in the YZ plane since as can be seen in Fig. 3, the principal stresses form a mutually perpendicular triad. The general procedure is to perform the matrix multiplication illustrated below which for the special stress state discussed above is

$$\begin{pmatrix} n_x & n_y & n_z \end{pmatrix} \begin{pmatrix} \sigma_x & 0 & 0 \\ 0 & \sigma_y & \tau_{yz} \\ 0 & \tau_{yz} & \sigma_z \end{pmatrix} = \begin{pmatrix} n_x\sigma & n_y\sigma & n_z\sigma \end{pmatrix} \quad (2)$$

where n_x, n_y and n_z are the direction cosines to one of the principal stresses and σ is the unknown value of the principal stress.

When equation (2) is expanded the following system of homogeneous linear algebraic equations results for the unknowns n_x, n_y, n_z

$$\begin{aligned} (\sigma_x - \sigma)\, n_x + 0\, n_y + 0\, n_z &= 0 \\ 0\, n_x + (\sigma_y - \sigma)\, n_y + \tau_{yz}\, n_z &= 0 \\ 0\, n_x + \tau_{yz}\, n_y + (\sigma_z - \sigma)\, n_z &= 0 \ . \end{aligned} \quad (3)$$

The well known relationship between the direction cosines is

$$n_x^2 + n_y^2 + n_z^2 = 1 \ . \quad (4)$$

The solution of equations (3) gives the values for the unknown direction cosines. The trivial solution in which all of the unknowns are zero is of no interest. Excluding such a solution, the determinant of the coefficients of (3) must vanish, a condition which leads to a cubic equation in σ, whose roots are the three principal stresses. In this special case, it is already known that σ_x is a principal stress, and its direction cosines will be (1, 0, 0). If σ is not equal to σ_x then $n_x = 0$ and equations (3) reduce to

$$(\sigma_y - \sigma)\, n_y + \tau_{yz}\, n_z = 0$$

$$\tau_{yz}\, n_y + (\sigma_z - \sigma)\, n_z = 0 \qquad (5)$$

with n_y and n_z not both zero. The characteristic equation of (5) is

$$\begin{vmatrix} \sigma_y - \sigma & \tau_{yz} \\ \tau_{yz} & \sigma_z - \sigma \end{vmatrix} = 0 .$$

Expanding the determinant and collecting terms gives

$$\sigma^2 - (\sigma_z + \sigma_y)\sigma + \sigma_y \sigma_z - \tau_{yz}^2 = 0 \qquad (6)$$

Equation (6) can be solved by applying the quadratic formula which gives two values for σ

$$\sigma_{\frac{1}{2}} = 1/2\,(\sigma_y + \sigma_z) \pm 1/2 \sqrt{(\sigma_z - \sigma_y)^2 + 4\tau_{yz}^2} . \qquad (7)$$

The orientation of the principal stress is computed as follows: Solving the equation involving σ_z of equation (5) for n_y gives

$$n_y = (\sigma - \sigma_z)\, n_z / \tau_{yz} .$$

Since n_x equals zero, (4) can be written

$$(\sigma - \sigma_z)^2 n_z^2 / \tau_{yz}^2 + n_z^2 = 1 .$$

Solving for n_z gives

$$n_z = \tau_{yz} / \sqrt{(\sigma - \sigma_z)^2 + \tau_{yz}^2} . \tag{8}$$

But

$$n_z = \cos \phi$$

where ϕ is the direction between the Z axis and the principal stress in question. By the trigonometric relations between tan ϕ and cos ϕ, (8) becomes

$$\tan \phi = \sigma - \sigma_z / \tau_{yz} . \tag{9}$$

The stress tensor also has the property that three quantities computed from it are invariant, meaning that these quantities are independent of the choice of coordinate axes. The three quantities are

$$I_s = \sigma_x + \sigma_y + \sigma_z$$

$$II_s = \sigma_x \sigma_y + \sigma_y \sigma_z + \sigma_z \sigma_x - \tau_{yz}^2 - \tau_{xz}^2 - \tau_{xy}^2 \tag{10}$$

$$III_s = \begin{vmatrix} \sigma_x & \tau_{xy} & \tau_{xz} \\ \tau_{xy} & \sigma_y & \tau_{yz} \\ \tau_{xz} & \tau_{yz} & \sigma_z \end{vmatrix} . \qquad \text{(10, cont'd)}$$

The first invariant is of particular importance. The mean normal stress acting at a point is defined as

$$\sigma_m = 1/3 \; I_s = 1/3 (\sigma_x + \sigma_y + \sigma_z) \qquad (11)$$

and because of its invariance can be expressed in principal stresses as

$$\sigma_m = 1/3 \; (\sigma_1 + \sigma_2 + \sigma_3) .$$

Now any state of stress at a point may be considered as a superposition of a spherical or hydrostatic stress state and a deviatoric stress or stress deviator. In the spherical stress tensor all shear components are zero and the three normal stress components are each equal to the mean normal stress σ_m . The components of the deviator stress tensor then differ from the stress tensor only in that σ_m is subtracted from each normal stress component. This is shown below where the first tensor is the stress tensor, the second is the spherical stress tensor and the third is the deviator stress tensor.

$$\begin{pmatrix} \sigma_x & \tau_{xy} & \tau_{xz} \\ \tau_{xy} & \sigma_y & \tau_{yz} \\ \tau_{xz} & \tau_{yz} & \sigma_z \end{pmatrix} = \begin{pmatrix} \sigma_m & 0 & 0 \\ 0 & \sigma_m & 0 \\ 0 & 0 & \sigma_m \end{pmatrix} + \begin{pmatrix} \sigma_x - \sigma_m & \tau_{xy} & \tau_{xz} \\ \tau_{xy} & \sigma_x - \sigma_m & \tau_{yz} \\ \tau_{xz} & \tau_{yz} & \sigma_z - \sigma_m \end{pmatrix}$$

The deviator stress tensor has three invariants as well as all of the other special mathematical properties of the stress tensor. It can easily be shown that the first invariant of the deviator is zero. Also by considerable algebraic manipulation it can be shown that the second invariant of the deviator is given by equation (12) when expressed in terms of principal stresses of the stress tensor.

$$II_{s'} = (1/6)\left[(\sigma_1 - \sigma_2)^2 + (\sigma_2 - \sigma_3)^2 + (\sigma_3 - \sigma_1)^2 \right] \quad (12)$$

For the reader who desires additional detail concerning any of the above concepts and derivations, the following references are suggested: (Hoffman and Sachs, 1953; Jaeger, 1956; Malvern, 1956; Timoshenko and Goodier, 1951.)

In theories of elasticity and plasticity (Hoffman and Sachs, 1953) the spherical stress is generally associated with volume change while the deviatoric stress governs change of shape. It would seem from the above and physical intuition that the volume strain of soil should be dependent only on the spherical stress tensor and independent of the deviator. Since the spherical stress tensor can be completely represented by the single scalar quantity σ_m, the relation between bulk density and the spherical stress tensor would then simplify to a single scalar equation involving only σ_m rather than a dependence on six stresses. This is the hypothesis proposed in this thesis as a soil compaction law: Mean normal stress is related to bulk density for all soils. It relates a scalar function of the forces acting on an element to a scalar function of the volume change of the element.

To prove the hypothesis two things must be demonstrated --

first, that mean normal stress does correlate with bulk density, and second, that deviatoric stress does not correlate with bulk density. The mean normal stress is the only measure of the spherical stress tensor. The deviator has many expressions which are measures of its intensity. Since the first invariant of the deviator is zero, the second invariant as given in equation (12) is perhaps the best over all measure. The maximum shear stress acting on an element is a function of the deviator and is given by

$$\tau_{max} = 1/2 \left(\sigma_{I} - \sigma_{III} \right) \tag{13}$$

where σ_I is the algebraically largest principal stress and σ_{III} is the algebraically smallest principal stress. The maximum shear is of special interest since the Coulomb-Mohr yield formula for soils deals with the shearing stress. The formula is

$$S = C + N \tan \theta \tag{14}$$

where S is the shearing stress on the plane of failure, C the cohesion of the soil, N the normal stress acting on the plane of failure and θ the angle of friction of the soil. The shearing stress predicted by the Coulomb-Mohr formula is not necessarily the maximum shearing stress at the point; the yield stress presumably approaches the maximum shearing stress and hence the interest. The maximum shear stress is an invariant of the stress state, i.e. independent of the choice of coordinate axes. The maximum normal stress which Soehne (1953) assumed to be related to bulk density is also a function of the deviator.

Like the maximum shear stress, the maximum normal stress is an invariant of the stress state. Thus if it can be shown that the mean normal stress is related to bulk density and that the maximum normal, the maximum shear and the second invariant of the deviator are not related to bulk density, then the hypothesis will be proved.

It is interesting that if a mean normal stress state is applied to a soil sample such as can be done with hydrostatic pressure, equations (12) and (13) reduce to zero since

$$\sigma_m \equiv \sigma_I \equiv \sigma_{II} \equiv \sigma_{III} .$$

Hydrostatic pressure compacts soil; hence it is unlikely that either the maximum shear or the second invariant of the deviator is related to bulk density.

The terms stress and pressure have both been applied to forces acting in soil. As implied above, pressure is the highly specialized stress state found in a fluid at rest. Hydrostatic pressure produces a truly spherical state of stress and such a state generally will not be found in soil. In this state, the stress vectors on all possible planes through a point are equal in magnitude to the pressure at the point. The directions of the stress vectors will be normal to all possible planes through the point. Therefore a typical cell would measure pressure at the point. In a general stress state, the stress vectors need not be the same in magnitude or direction for every plane through a point. For such a stress state, the typical cell measures the normal component of the stress vector which is by definition the normal stress on the plane. The normal stress is not necessarily equal to the pressure, mean normal stress, acting at the point.

FIELD TESTS

Theory.

Since the principal directions of the stress state are not generally known, six quantities need to be determined to define stress at a point. Only four quantities need to be measured if a special stress state such as discussed in the previous section is considered. When surface loads are symmetrically distributed with respect to a line of symmetry, the vertical plane containing that line is a principal plane of stress. That this is true can be seen by reasoning as follows: If the forces are symmetrically distributed, the forces acting on one side of the plane of symmetry must be equal to the forces acting on the other side of the plane. The conclusion is that only normal forces can act on the plane since no shearing forces are present. Hence, the plane must be a principal plane of stress since by definition a principal plane has only normal stress acting on it. If, in addition, the surface loads have circular symmetry, the stress state has rotational symmetry about a vertical axis through the center of the load circle and any plane containing this axis is a principal plane. Fig. 4 shows a loading symmetrically distributed over a circle. The Z axis is the vertical axis of symmetry and the YZ plane is a typical plane of symmetry and therefore a principal plane. The stress state at any point in the plane of symmetry will be as in Fig. 5.

At the present time no sensing elements are available for

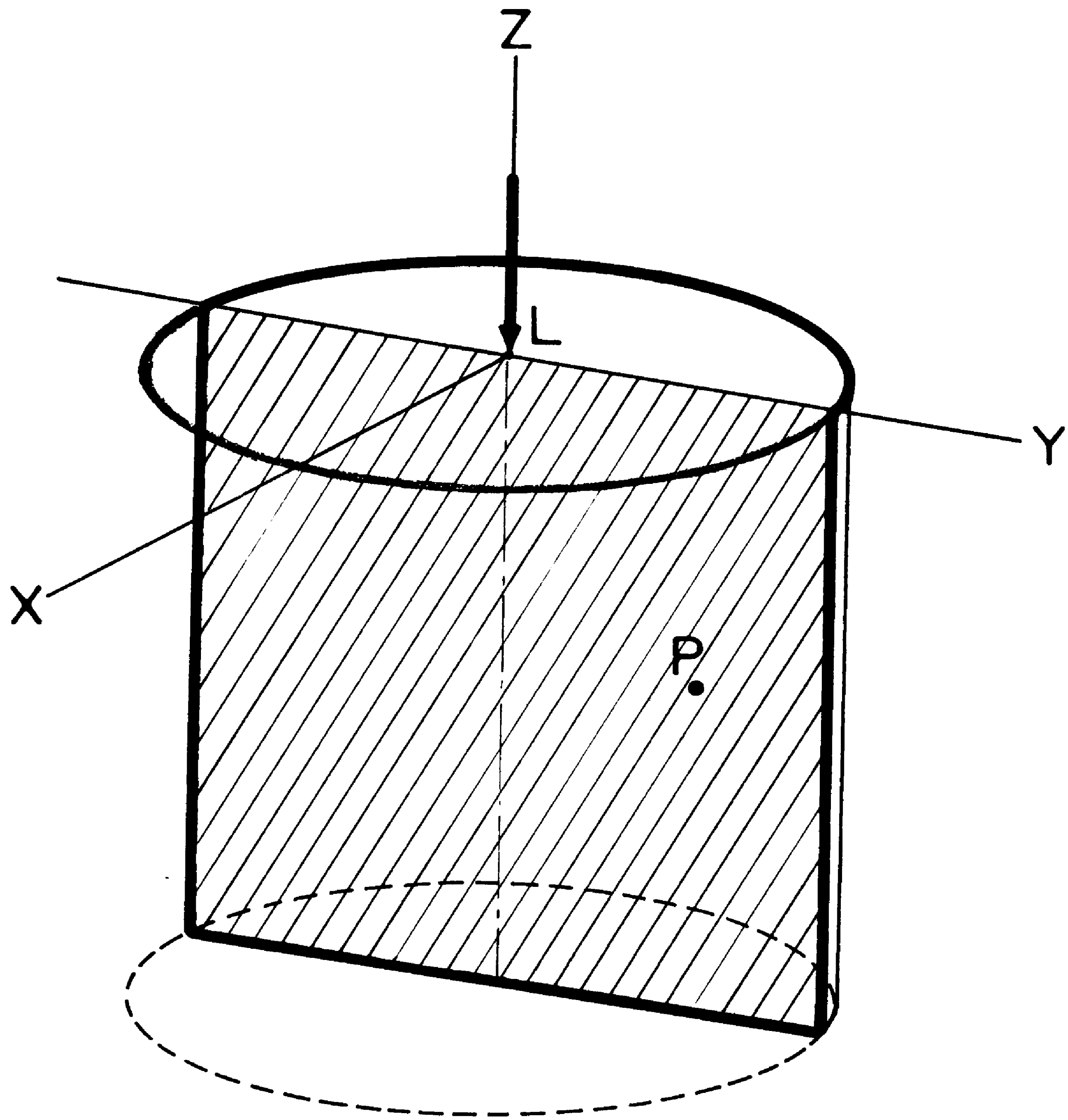

FIG. 4 PLANE OF SYMMETRY UNDER A CIRCULAR LOAD

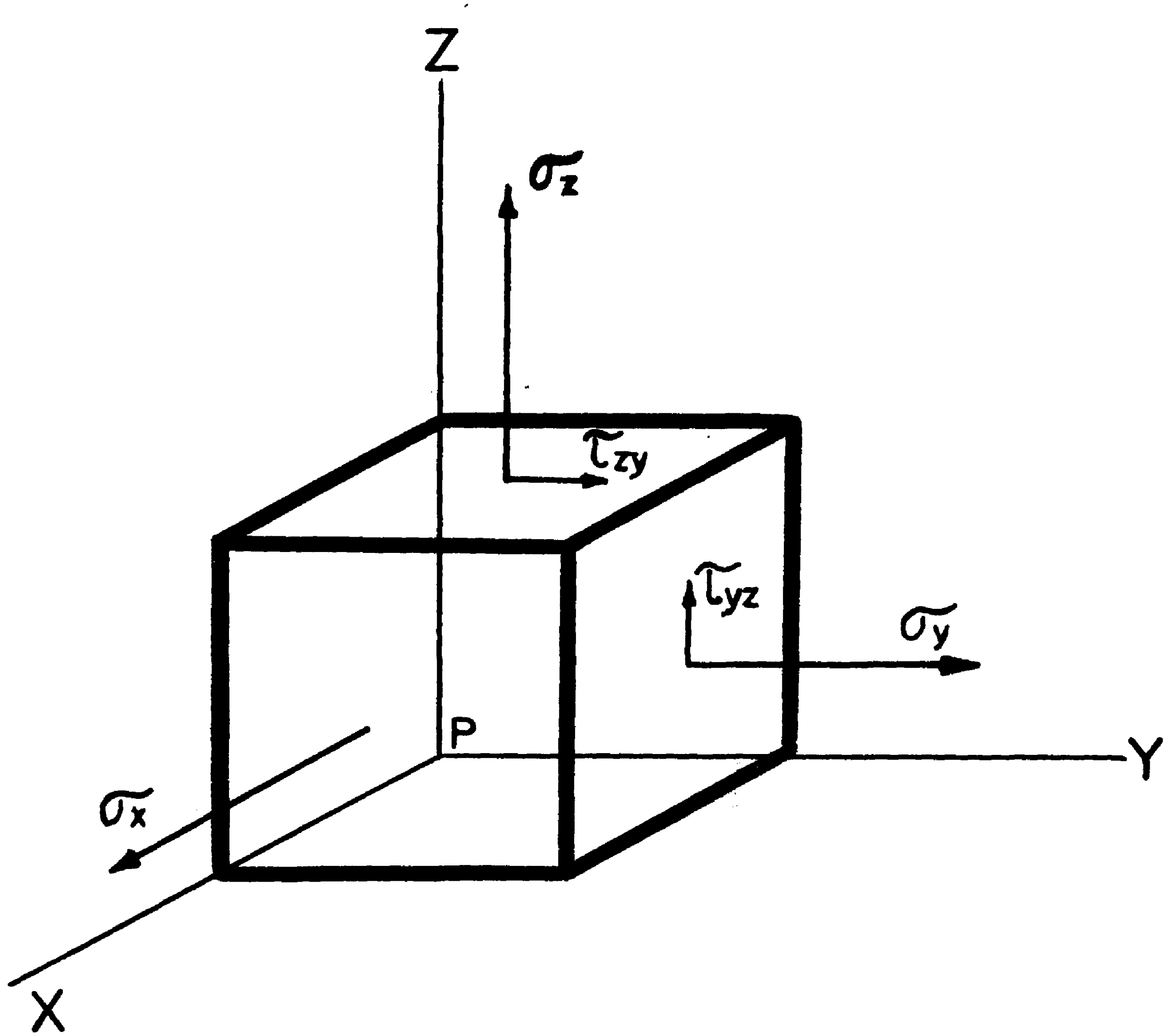

FIG. 5 STRESSES ON VOLUME ELEMENT IN A PLANE OF SYMMETRY

measuring shearing stresses. The unknown shearing stress, τ_{yz} in Fig. 5 can be calculated by using equation (1). Note that the stress state used in deriving equation (1) is precisely the stress state shown in Fig. 5. Hence by measuring σ_x, σ_y, σ_z, and the normal stress σ_n on a plane whose normal bisects the positive Y and Z axes and lies in the YZ plane, the stress tensor acting at any point in a plane of symmetry can be determined.

The four measurements above must be made at the same point in order to determine the stress tensor at the point. The measurements can be made by appealing to the rotational symmetry under a circular load. The same stress state acts at any point on the circumference of a horizontal circle centered on the axis of symmetry. The uniform stress state is true for a homogeneous soil since from rotational symmetry each point on the concentric circle is subject to the same forces. Four stress cells (Cooper, et. al., 1957) can be oriented on a circle to measure the stress tensor as shown in Fig. 6. In Fig. 6 by imagining the cells rotated around the circle until they all rest at one point P, it can be seen that the cell normals labeled σ_x, σ_y, and σ_z will be mutually perpendicular while σ_n will make equal angles of 45 degrees with the Y and Z axes and a 90 degree angle with the X axis. By also measuring the bulk density at the points labeled B, a method is provided to measure both the stress tensor and bulk density 'at the same point.'

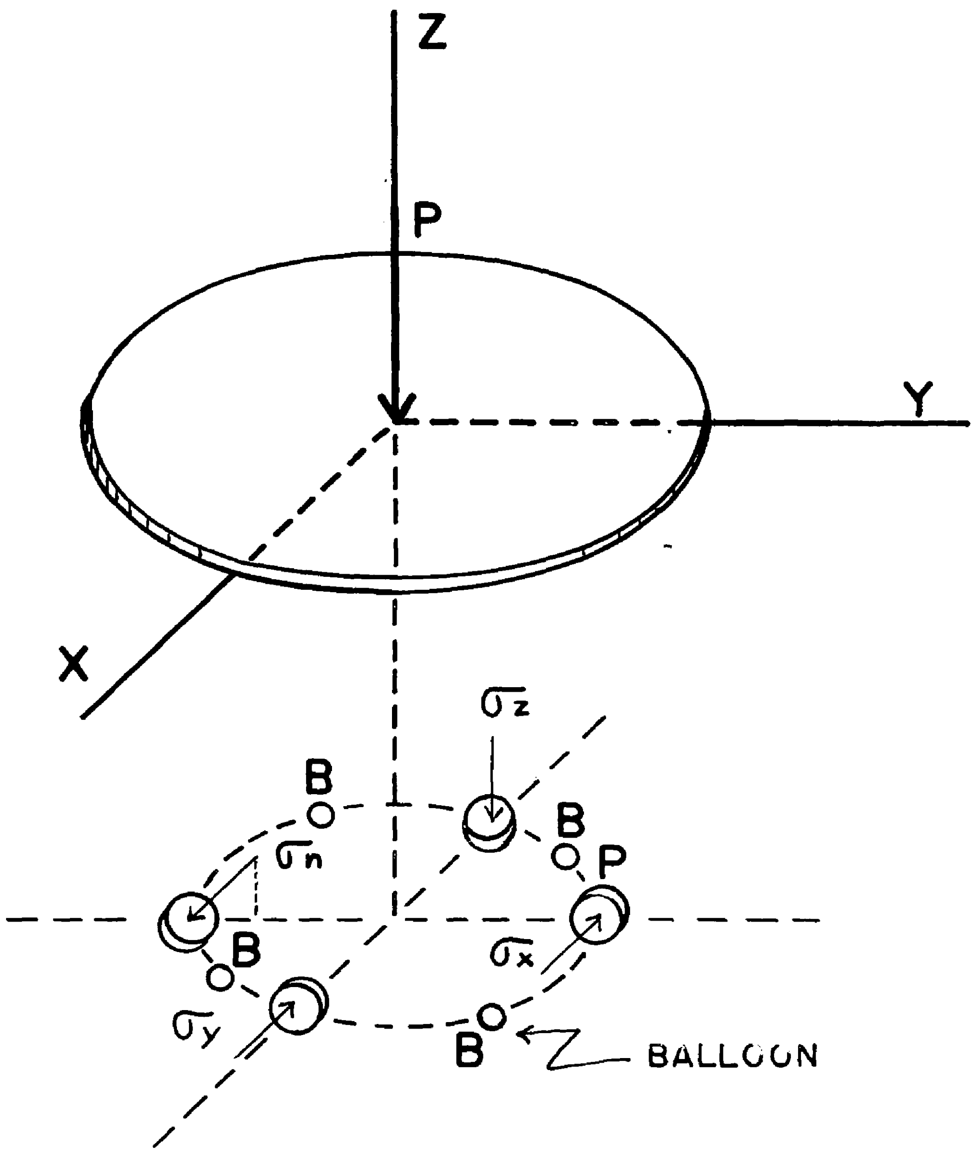

FIG. 6 CELL ORIENTATION

Indicating Volumeter.

A review of accepted methods for measuring bulk density (Russell and Belcerek, 1944; Torstensson and Erickson, 1936; Veihmeyer, 1929) revealed that they would not be acceptable for the experiment indicated above. All methods required a large sample compared with the volume of the soil in the immediate vicinity of the stress cells. Since a distribution of bulk density would be expected, considerable error would result. Furthermore, because a soil sample had to be removed, only one stress-bulk density measurement could be made for a given test set up. This would make testing very time consuming. The requirements of the above objectives were met by developing an indicating volumeter.

Briefly, the volumeter consists of a capillary tube connected to a non-collapsible plastic tubing. The plastic tubing is in turn connected to a small balloon (approximately 15 cc.). When the balloon, filled with soil, is surrounded with a large volume of soil of the same type, the volume of the balloon can be considered a point mass. As the soil compacts, the bulk volume of the soil decreases and the air in the balloon is forced out. The decrease in volume of the balloon is measured by recording the displacement of a mercury bubble in the capillary tube. The volume per linear unit of the capillary tube is easily determined. The volumeter permits measuring the volume change at a point in the soil over a range of bulk density without disturbing the soil sample until the test is completed. The final volume of the soil sample is determined by weighing in and out of water.

The principle of the volumeter was checked using two soil types in a soil box. Three of the balloons were placed in the center of a box containing six inches of soil and a uniform load was applied over the entire surface. The change of volume of the soil in the box was determined by measuring displacement of the plunger. From the initial weight and moisture content of the soil in the box, the average bulk density of the soil could be computed. This average was compared with the average given by the indicating volumeter. The results of this test are shown in Table A.

Table A

Comparison of Indicating Volumeter and Soil Box Bulk Densities in Two Soil Types

Maumee Sandy Loam		Clay	
Soil box gm/cc	Indicating Volumeter gm/cc	Soil Box gm/cc	Indicating Volumeter gm/cc
1.14	1.16	1.24	1.24
1.20	1.19	1.31	1.29
1.26	1.24	1.37	1.35
1.33	1.29	1.44	1.41
1.39	1.36	1.51	1.48
1.45	1.43	1.57	1.55
1.52	1.52		

The only question about the principle of the volumeter is whether the balloon membrane interferes with the equilibrium between the soil inside and outside the balloon. The data indicate the balloon membrane does not interfere. Hovanesian (1958) further developed the volumeter by making it recording as well as indicating, and his studies give an additional test of the principle.

Apparatus.

The facilities of the National Tillage Machinery Laboratory, Auburn, Alabama, were made available to conduct the tests. Eleven different soils types are arranged in bins so that the soil can be prepared mechanically; in addition, other laboratory equipment for making physical measurements of soil properties enabled a maximum of information to be obtained with a minimum of time and effort. All data were taken with these facilities. The stress cell used was similar to the type presented by Cooper, et.al. (1957.) Multi-channel recording oscillographs with appropriate strain gage amplifiers were used to record cell readings. The bulk density was measured by reading the indicating volumeter shown in Fig. 7. The weight and the final volume of soil in the balloons were obtained using a small scale accurate to 0.01 gm. This is shown in Fig. 8. The loading plate (20 in. in diameter) and the method of applying the load are shown in Fig. 9. The large power car of the Laboratory was clamped to the rails of the soil bins to provide the necessary support for applying the load.

Procedure.

The soil was prepared by rotary tilling to the depth of the soil bins (approximately 24 in.) It was left in this loose condition for the tests. The soil was moistened either before or after tilling depending

Fig. 8 Method of weighing in water

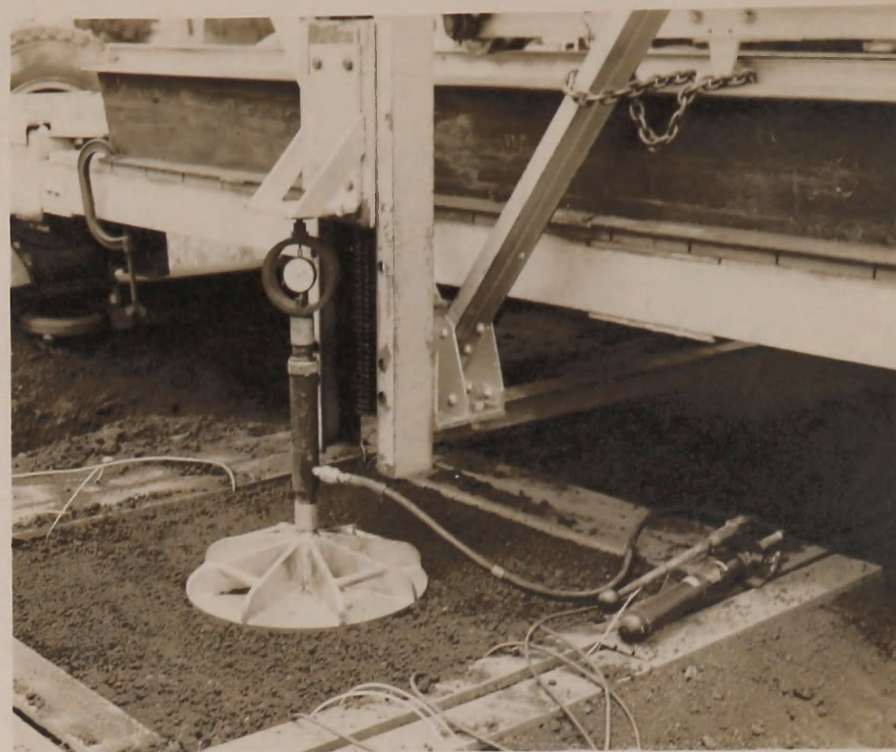

Fig. 9 Method of loading

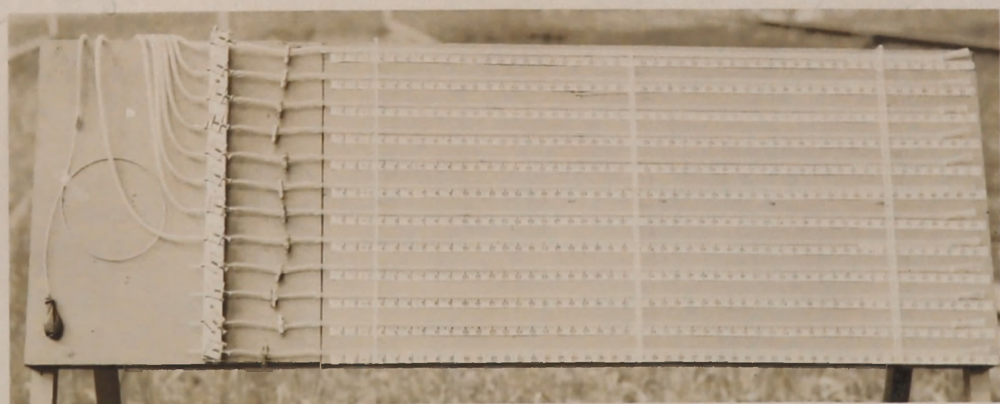

Fig. 7 Indicating volumeter

upon soil type and convenience in manipulating the soil. This treatment left the soil in a nearly homogeneous state.

To conduct a test, a platform was placed on the loose soil and an area four feet square excavated to the depth of the bins. The soil was replaced by hand as carefully as possible to the desired depth and leveled with a template. The cells and balloons were then positioned as shown in Fig. 6 and 11. The remaining soil was then replaced and again leveled. The loading plate was properly positioned and the instruments were connected. The data were taken at prescribed intervals between 0 and 26.5 psi. The general view of the test set up is shown in Fig. 10. Upon completing a test, the cells and the balloons were removed and the balloons weighed in and out of water to determine their final volume. The equipment was moved to a new area to conduct the next test. The moisture content and other physical properties of the soils tested are given in Table B.

Results.

To properly test the mean normal stress-bulk density hypothesis or any other hypothesis, different stress states must be applied to a volume element; if different stress states are not used, only proportional loading results. In proportional loading, all of the stress tensor components are linearly related to the applied load. The linearity means that all of the invariants of the stress tensor will be linearly related and consequently all of the invariants will appear to be

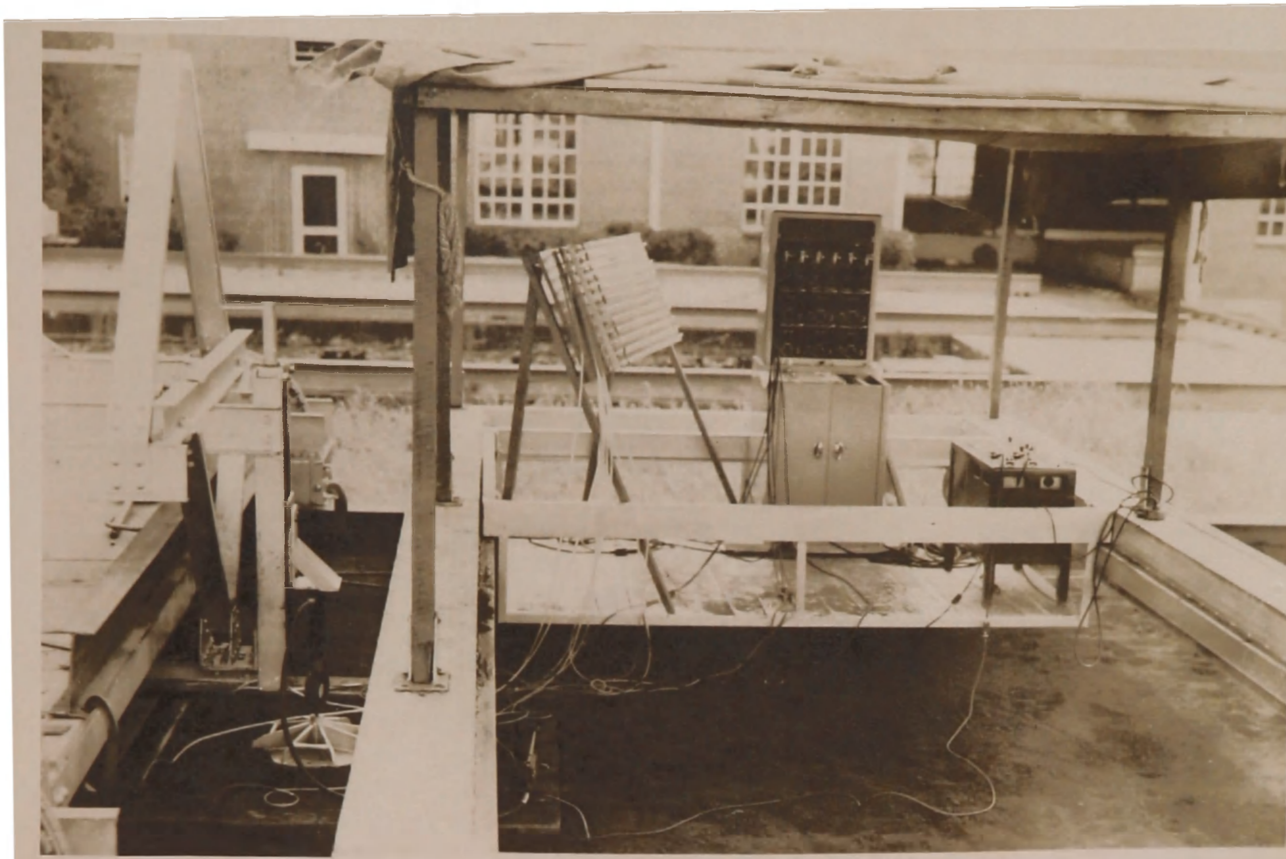

Fig. 10 General view of test equipment (above)

Fig. 11 Cell orientation (below)

Table B

PHYSICAL PROPERTIES OF
SOILS USED IN TESTS

(Below in % organic free material)

	Hiwassee Sandy Loam	Decatur Silty Clay Loam	Lloyd Clay
Gravel	0.1	1.2	1.5
Very coarse sand	2.0	0.4	2.2
Coarse sand	19.5	1.6	4.3
Medium sand	23.3	2.6	3.7
Fine sand	25.4	8.4	7.4
Very fine sand	2.9	5.8	5.6
Total silt	10.9	54.9	17.2
Fine silt	8.3	32.7	11.2
Clay	16.0	26.3	59.6
(Below in % moisture)			
Lower plastic limit	13.03	17.67	32.08
Plasticity index	6.51	11.07	24.29
15 atm. tension	5.5	10.0	22.5
Average moisture content of soil during tests	9	16	19

related to bulk density. Different stress states were obtained by varying the location of the cell and balloon circles. Preliminary tests indicated that the best variations obtainable under the 20 in. diameter loading plate were as follows:

1. A 12 in. diameter circle initially 5 in. below the loading plate.
2. A 12 in. diameter circle initially 12 in. below the loading plate.
3. An 18 in. diameter circle initially 18 in. below the loading plate.
4. A 20 in. diameter circle initially 18 in. below the loading plate.

Five replications at each stress state were taken and the results are reported in Tables I through XII in the Appendix. The bulk density readings reported are an average of the four measurements taken around the circle.

The chosen measures of the spherical and deviator tensors were computed from the four measured stress values using the appropriate formulae, namely equations (7), (11), (12) and (13). The algebraically ordered principal stresses were determined using equation (7) and the measured value of σ_x. The largest value for σ from equation (7) gave σ_I. The smallest value from equation (7) or σ_x gave σ_{III} depending upon which was the smaller value. It should be noted that in all calculations a compressive stress has been considered positive whereas usually the positive sense is reserved for tension forces; hence negative stresses in Tables I through XII indicate tensile stresses in the soil. Equation (9) was used to calculate the angle ϕ. The largest principal stress σ_I was substituted for σ so that ϕ represents the angle between the Z axis and the largest principal stress σ_I. Since the orientation of σ_x is known and it is one of the principal stresses, ϕ completely determines the orientation of the triad of principal stresses. MISTIC, an electronic digital computer at Michigan State University, was used to make the lengthy calculations involved in evaluating the above equations.

There were several sources of error in the experiment. The assumption that each cell would be subjected to the same stress state on one of the concentric circles is not completely true. This was revealed by variation in bulk density readings around the circle and by comparison of the readings and orientations of cells whose normals were in the YZ plane. An example of the extreme variation observed in four bulk density readings around a circle for a 26.5 loading in Hiwassee soil is: 1.56, 1.53, 1.58, 1.49. The average spread of four bulk density readings for all tests was approximately .04 gm/cc. Additional error occurred during certain tests when some of the cells rotated from their original orientations. In cases where the rotation was more than 10°, the rotated cell reading was corrected by adjusting it closer to the average of cells which measured the same stress component but did not rotate. While this is highly arbitrary, it was necessary on only 10 of the 480 total readings. Finally, there was the variability of the soil itself. The magnitude of soil variation due to the fortuitous structure of the soil has never been evaluated but experience dictates that it is probably much larger than any of the above errors. Furthermore, some of the variation in cell readings and bulk density readings was probably due to soil variation rather than errors in experimental procedure.

The variation which can be seen by examining the data in Tables I through XII requires that some method of statistical analysis be employed. A plot of any of the computed values such as $\overline{\sigma_x}$ or $\overline{\sigma_I}$ results in a straight line when the stress is plotted on a logarithmic axis and bulk density on the linear axis. This exponential relationship has been observed by other investigators (Soehne, 1953; Hovanesian, 1958.) The straight line plot offered a simple graphical method for averaging the data and obtaining an estimate of the standard error. The best fitting straight line was drawn and adjusted slightly until the total distances from the points on each side of the line were equal. This procedure located the average line with a reasonable degree of accuracy and could be carried out very rapidly. Assuming a normal distribution of error, one standard error would include 68.3% of the plotted points. Thus the standard error lines were located so that approximately 68.3% of the plotted points fell between the two standard error lines. An example of this procedure is shown in Fig. 12. It is admitted that the procedure of averaging and determining standard error is not statistically precise, but it is rapid and does give an estimate of variation which is reasonably meaningful.

FIG. 12 STANDARD ERROR AND AVERAGE OF MEAN STRESS VERSUS BULK DENSITY

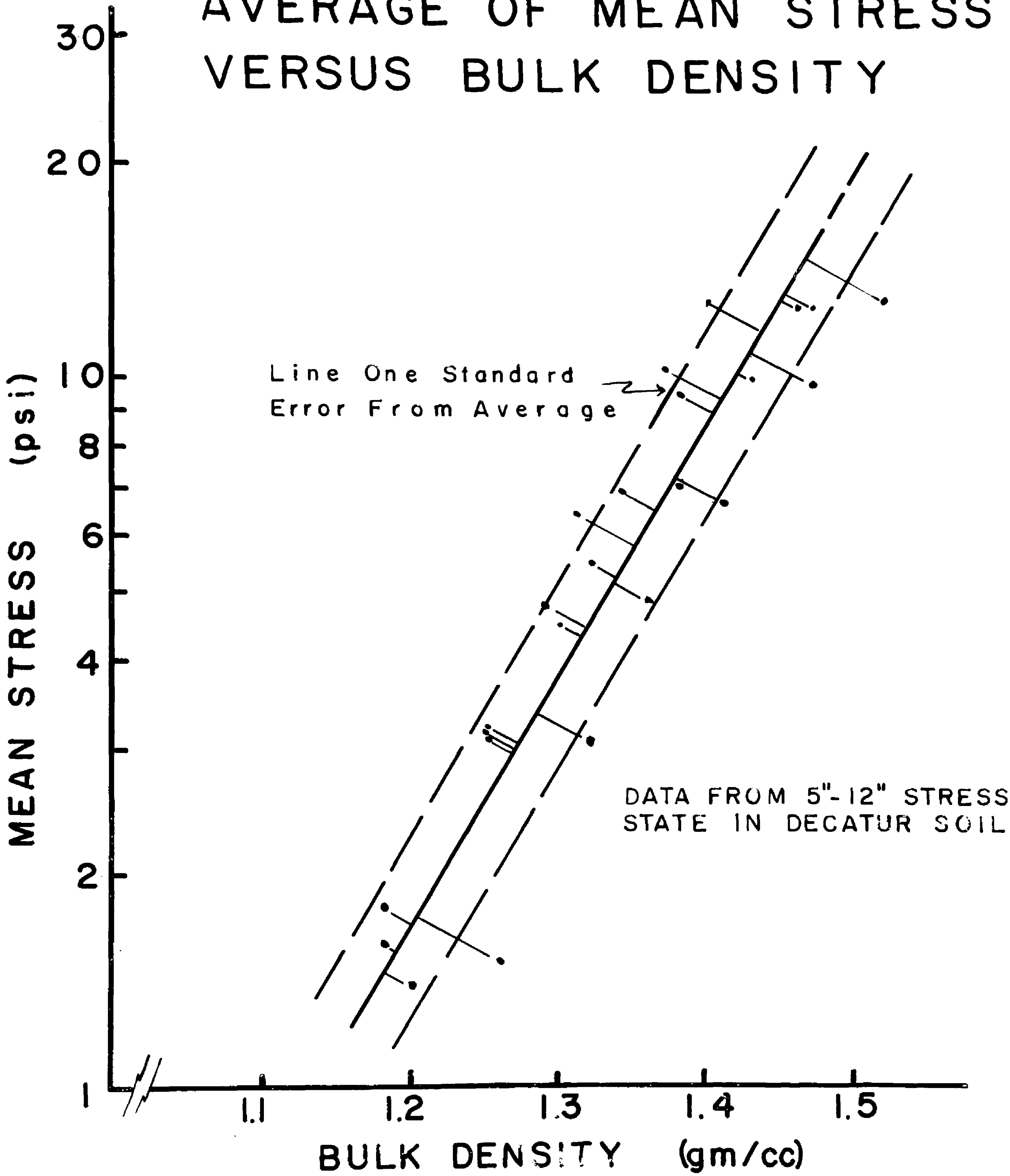

The four measures of the spherical stress tensor and the deviator stress tensor - namely σ_m, σ_I, II_s, and τ_{max} - were averaged individually using the procedure shown in Fig. 12 for each stress state and each soil type. Their individual standard error was also determined and the results summarized in Fig. 13 through 24. If a quantity is related to bulk density in a general manner, the average lines from each different stress state should not be significantly different for a given soil. Figures 13, 14, and 15 indicate no significant difference for the mean normal stress in all three soil types. Similarly, if a quantity is not related to bulk density in a general manner, the average lines from each different stress state should be significantly different for a given soil. Figures 16 through 24 show that σ_I, τ_{max} and II_s, are not all significantly different. Thus based upon the data, it cannot be determined whether compaction is independent of the deviator. Furthermore, because of the large variation, mean normal stress is not clearly related to compaction. Figures 13 through 24 reveal, however, that of the four invariants investigated, the mean normal stress is the best invariant to relate to bulk density.

The data indicates that for a given measured stress state (location of a circle), the magnitude of the principal stresses is very nearly independent of soil type. To obtain a physical picture of the average stress states measured at the four locations of circles, the three principal stresses for the 26.5 psi loading in all soil types were

FIG. 13 MEAN NORMAL STRESS VS BULK DENSITY IN HIWASSEE SOIL

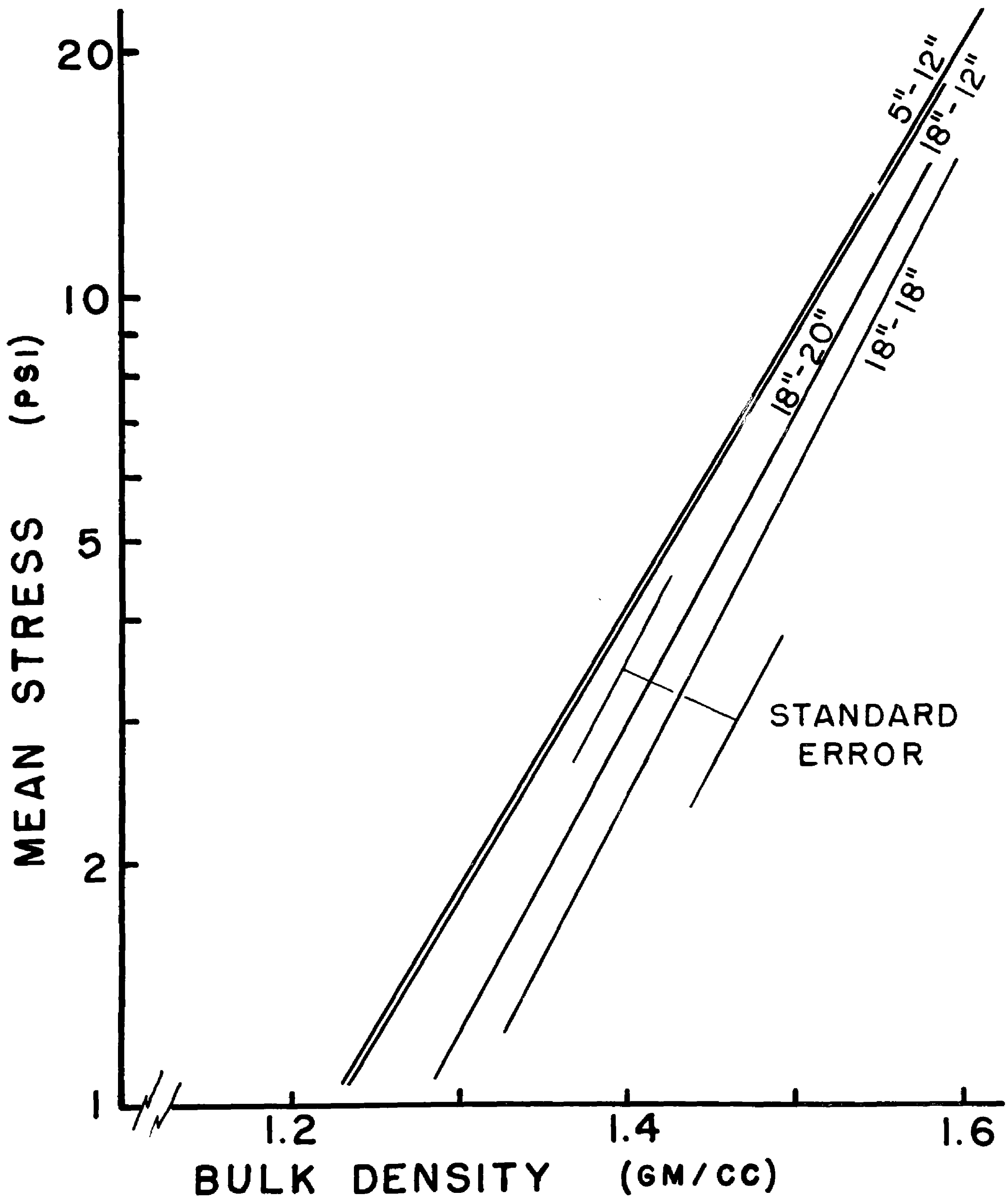

FIG. 14 MEAN NORMAL STRESS VS BULK DENSITY IN LLOYD SOIL

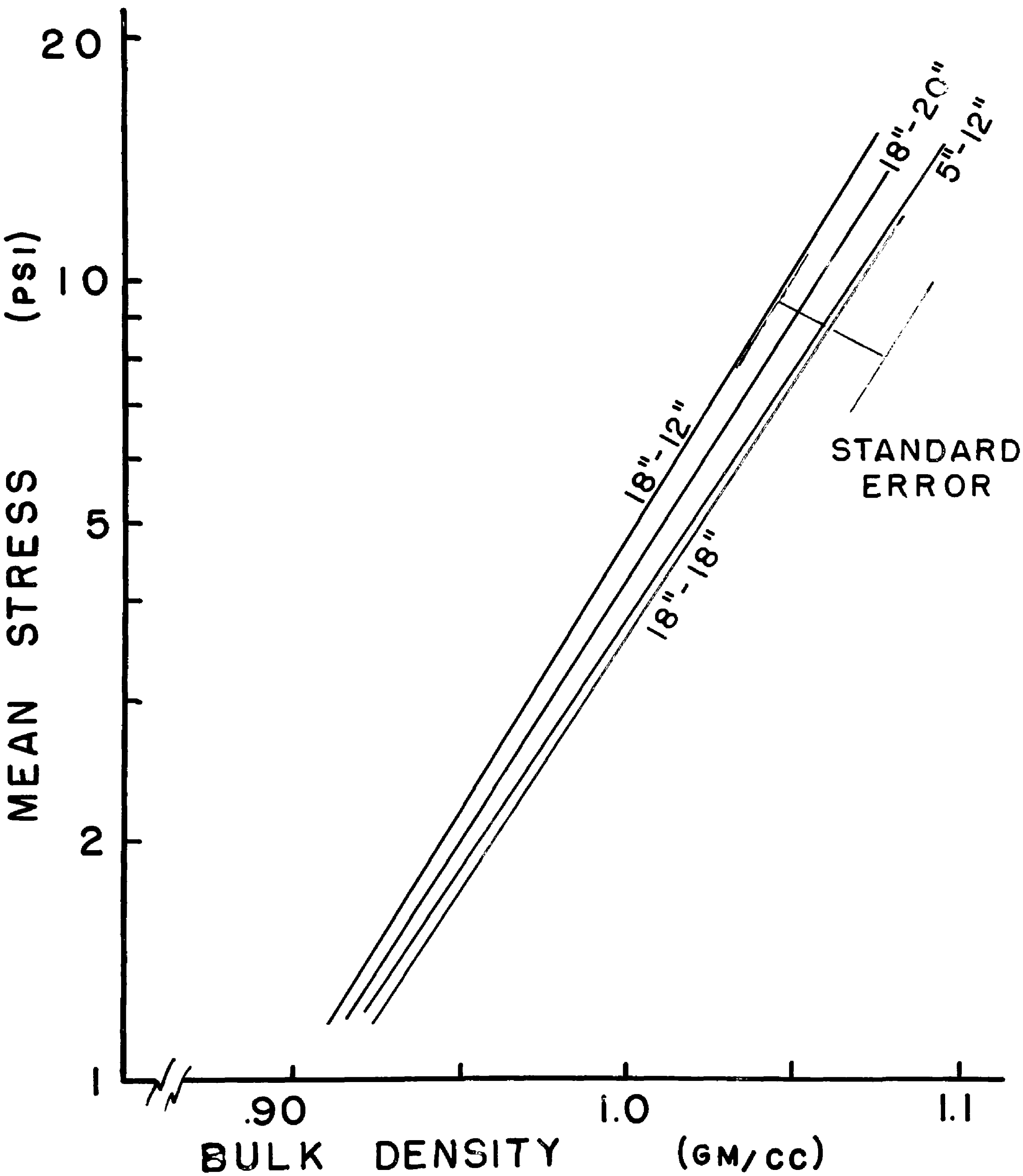

FIG. 15 MEAN NORMAL STRESS VS BULK DENSITY IN DECATUR SOIL

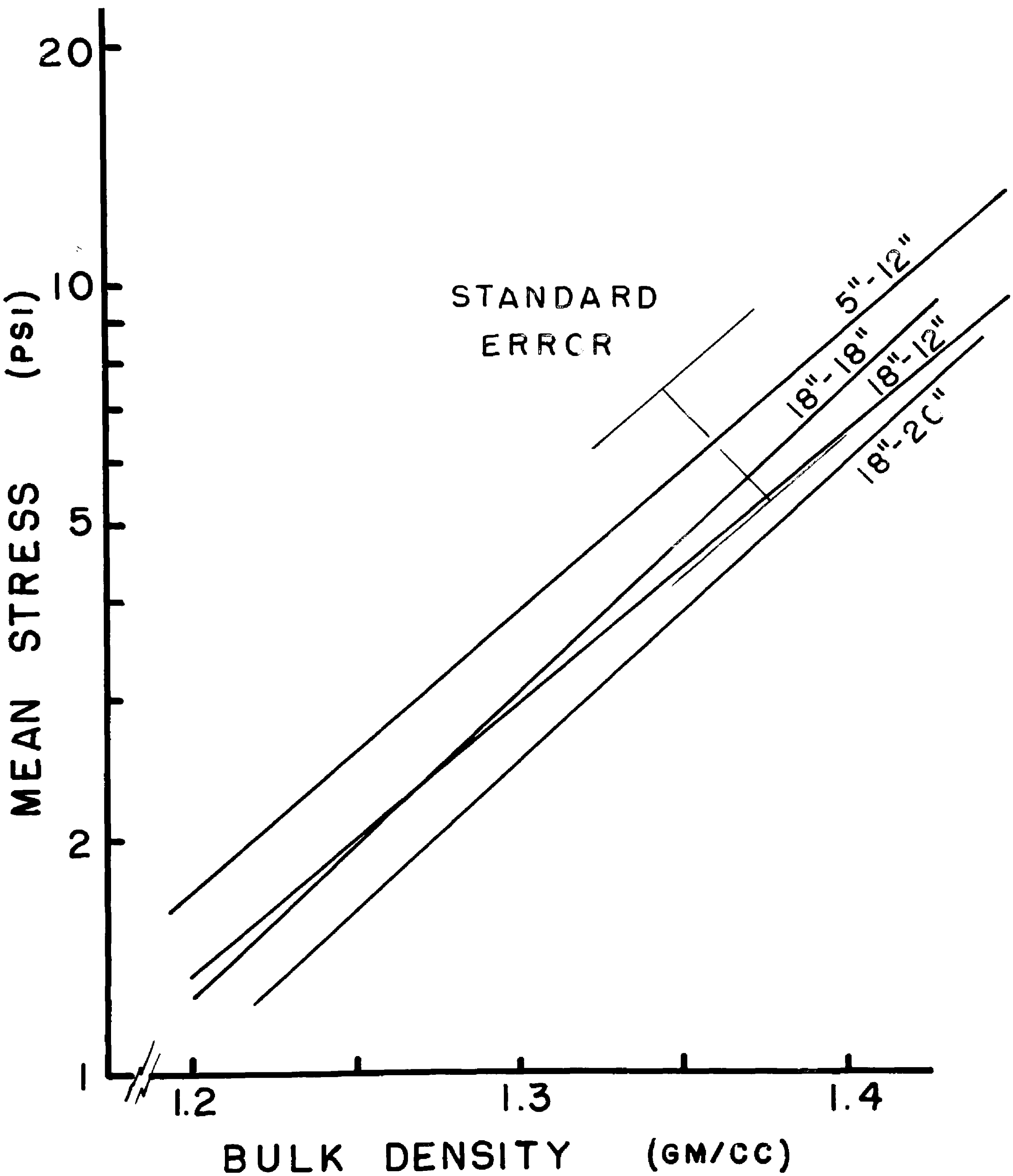

FIG. 16 MAXIMUM NORMAL STRESS VS BULK DENSITY IN HIWASSEE SOIL

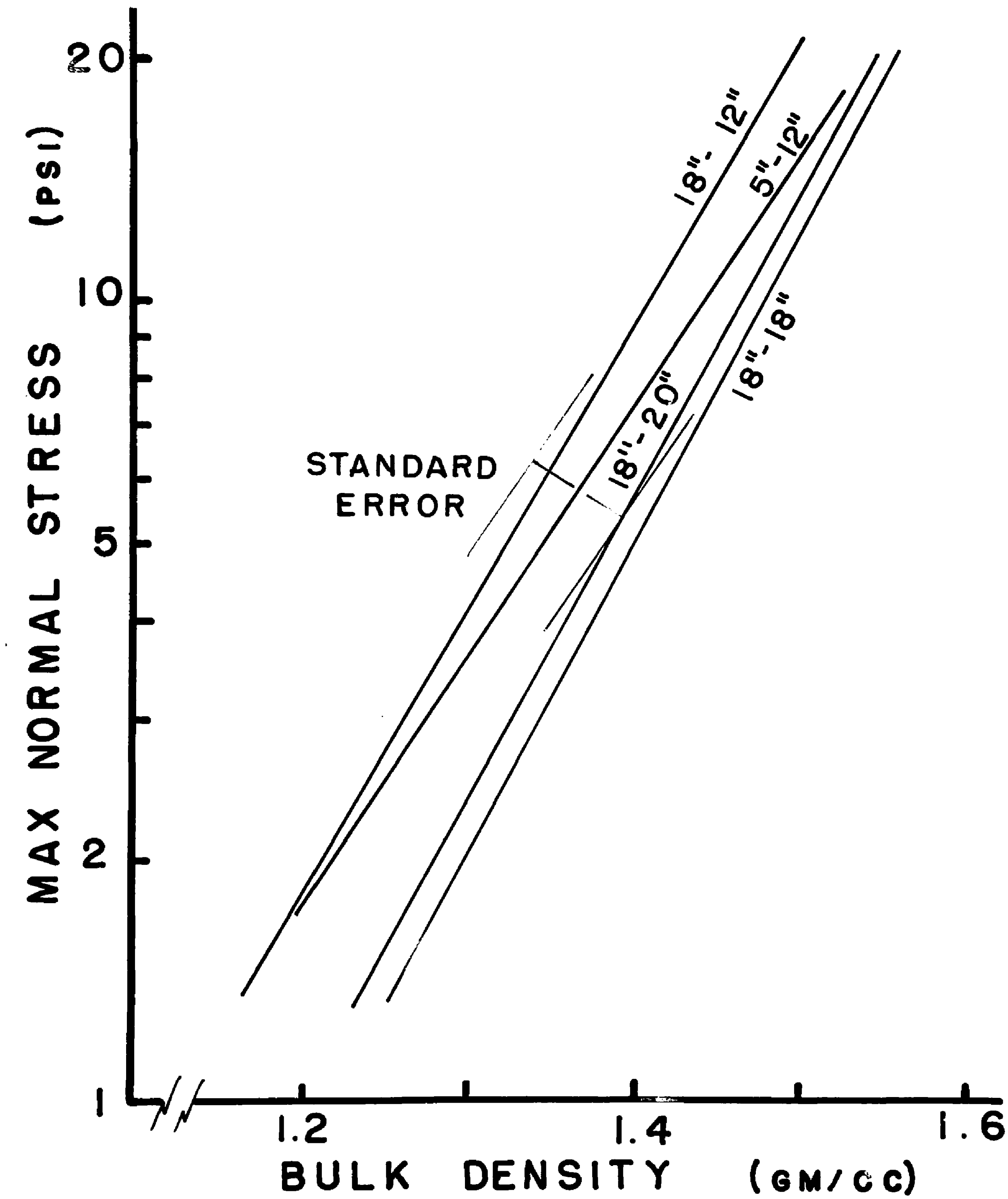

FIG. 17 MAXIMUM NORMAL STRESS VS BULK DENSITY IN LLOYD SOIL

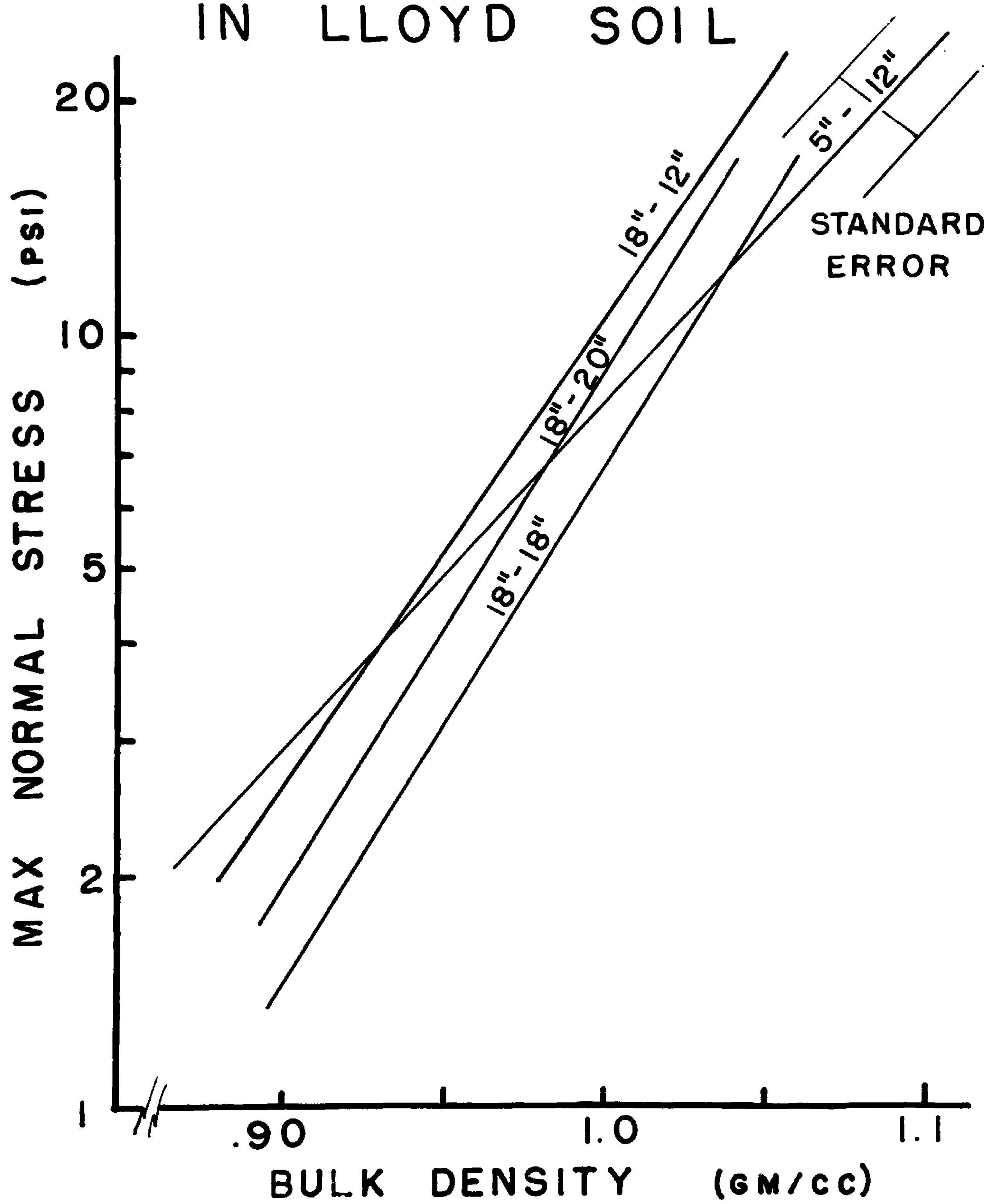

FIG. 18 MAXIMUM NORMAL STRESS VS BULK DENSITY IN DECATUR SOIL

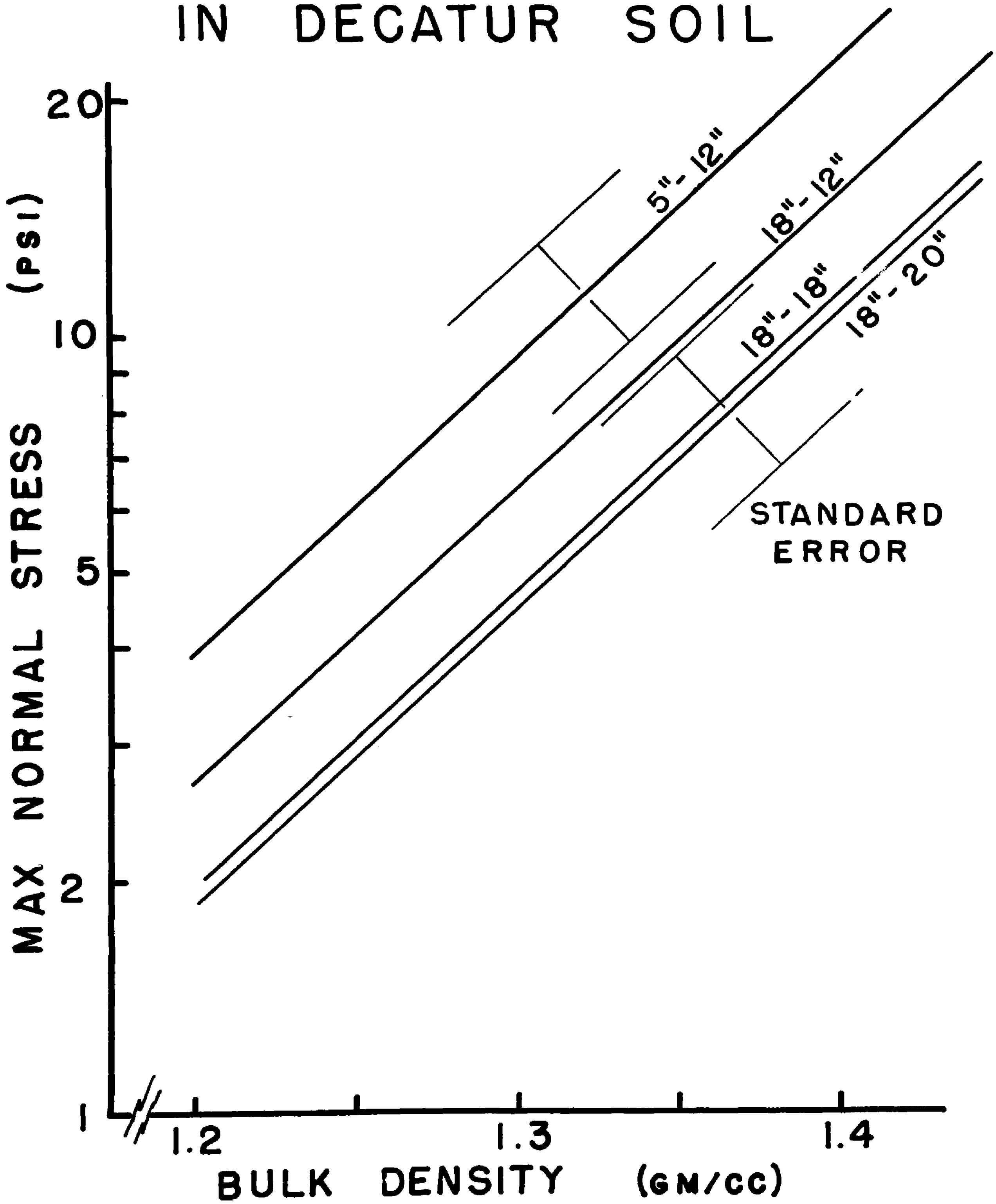

FIG. 19 MAXIMUM SHEARING STRESS VS BULK DENSITY IN HIWASSEE SOIL

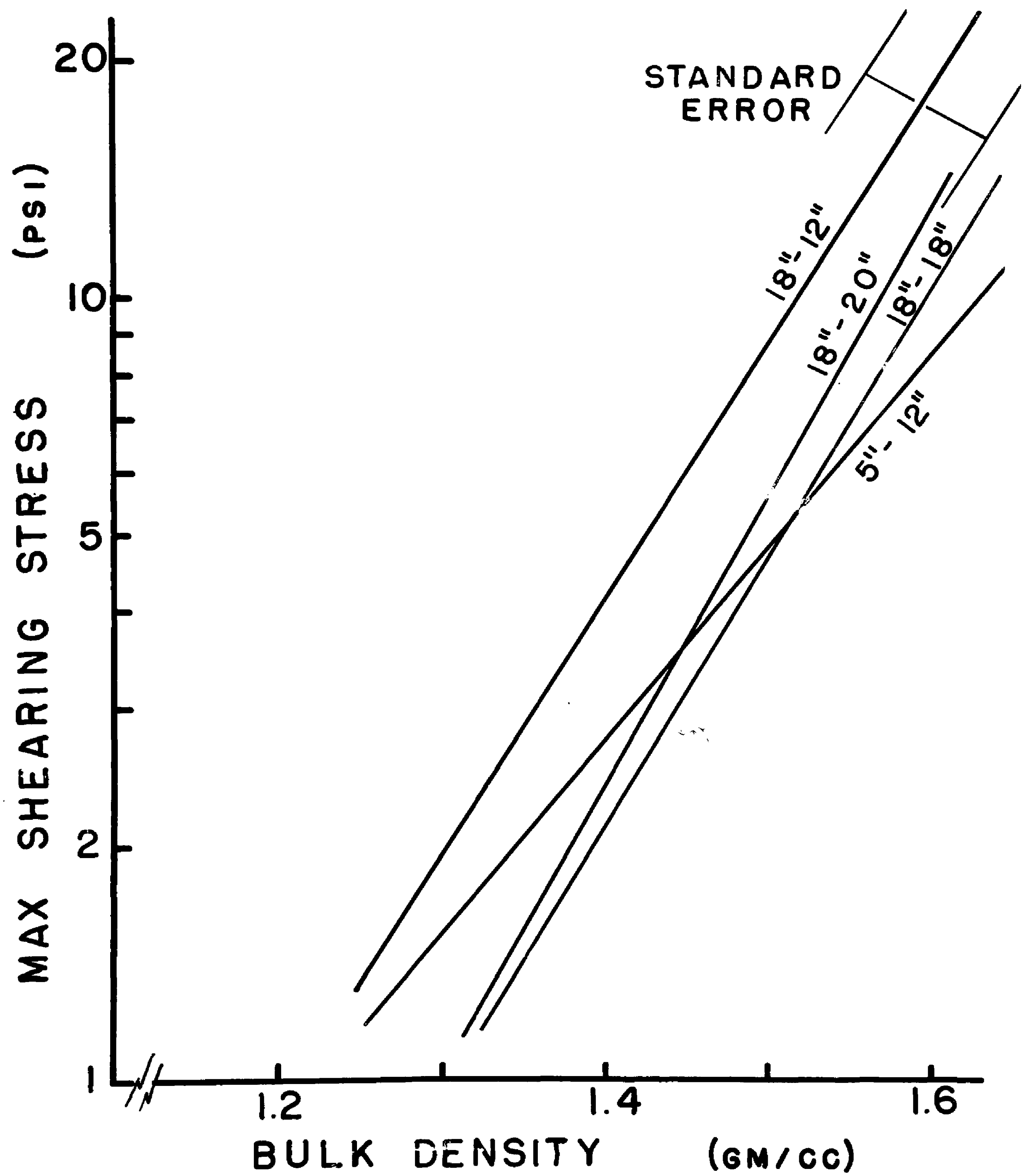

FIG. 20 MAXIMUM SHEARING STRESS VS BULK DENSITY IN LLOYD SOIL

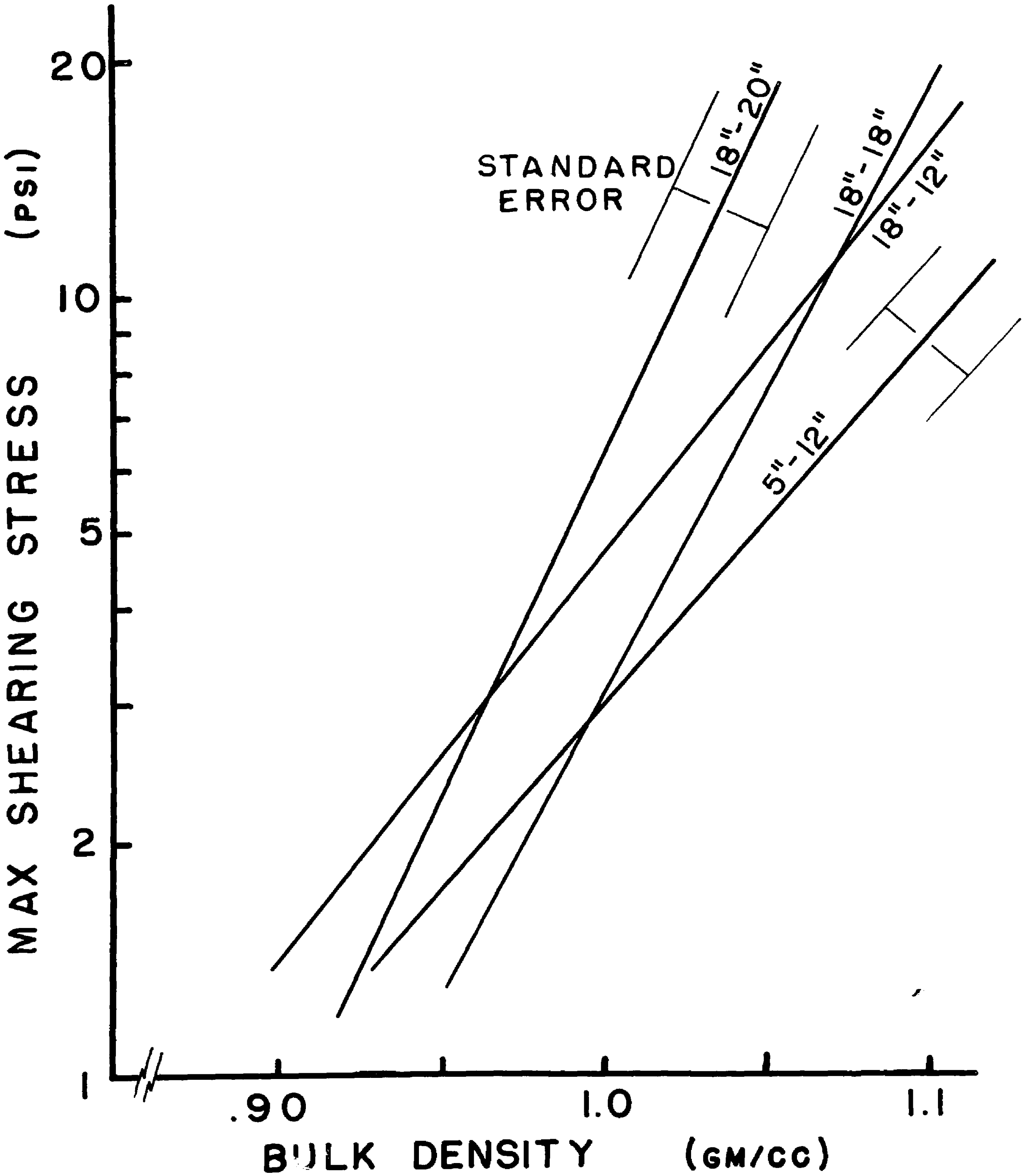

FIG. 21 MAXIMUM SHEARING STRESS VS BULK DENSITY IN DECATUR SOIL

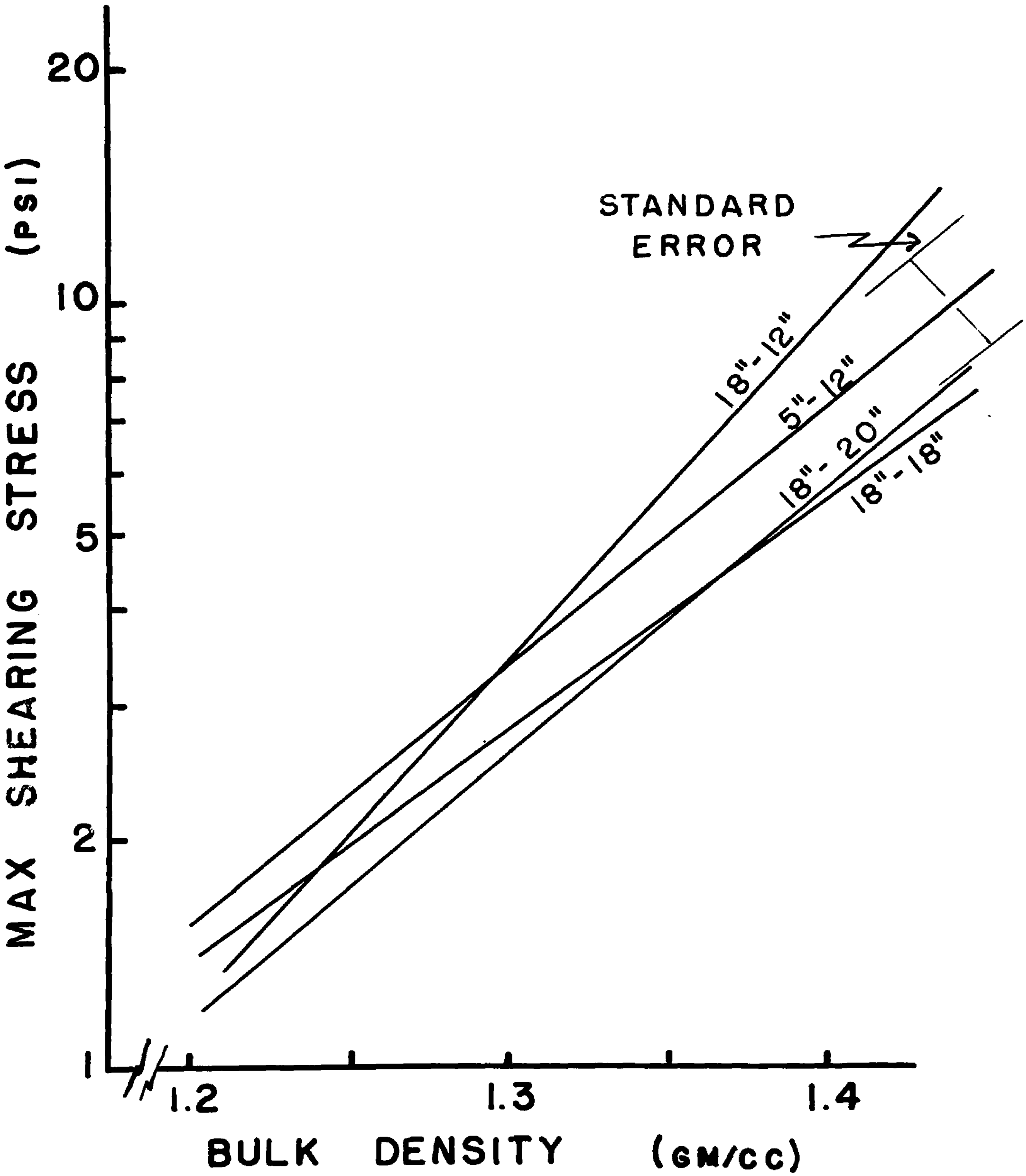

FIG. 22 SECOND INVARIANT OF DEVIATOR VS BULK DENSITY IN HIWASSEE SOIL

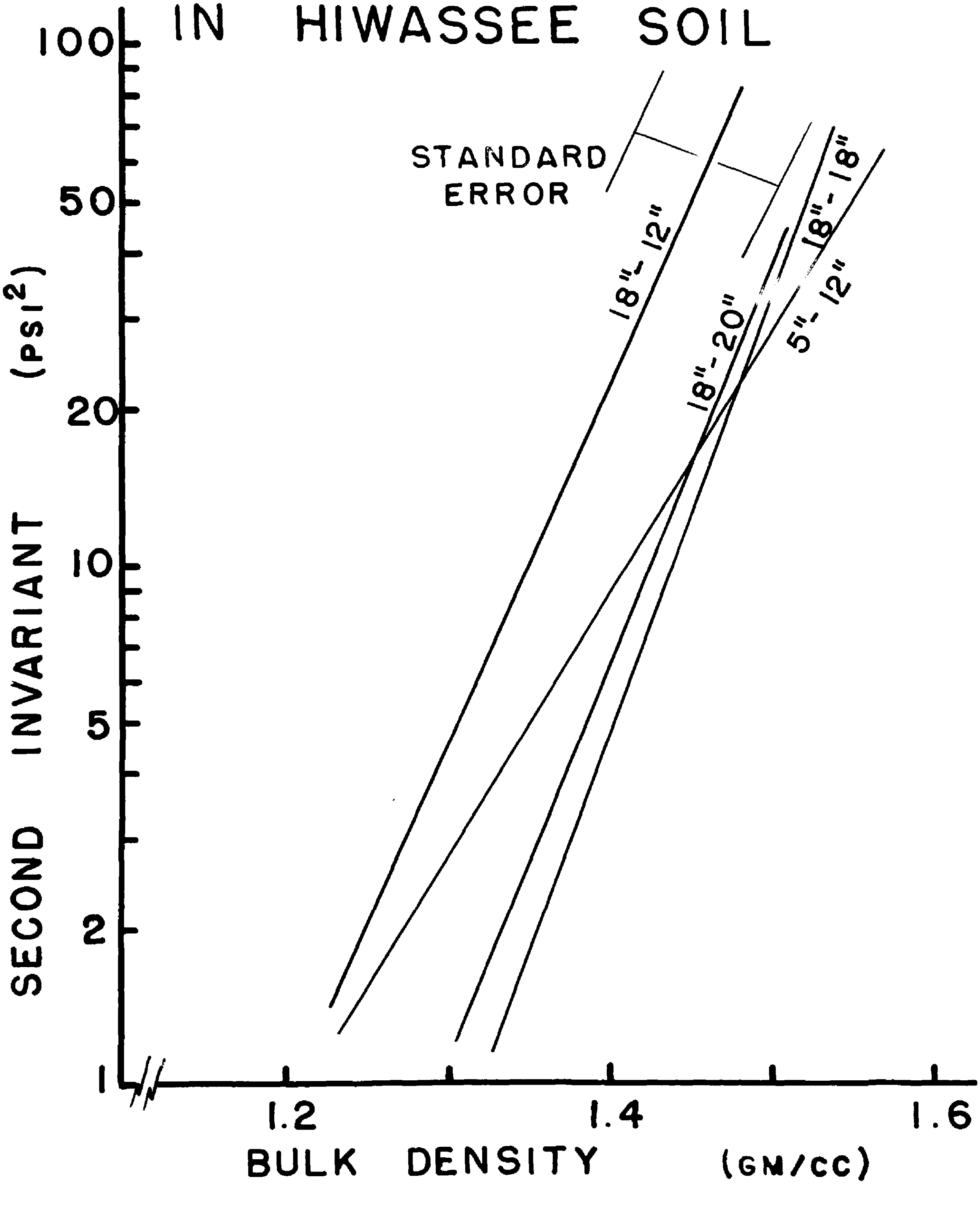

FIG. 23 SECOND INVARIANT OF DEVIATOR VS BULK DENSITY IN LLOYD SOIL

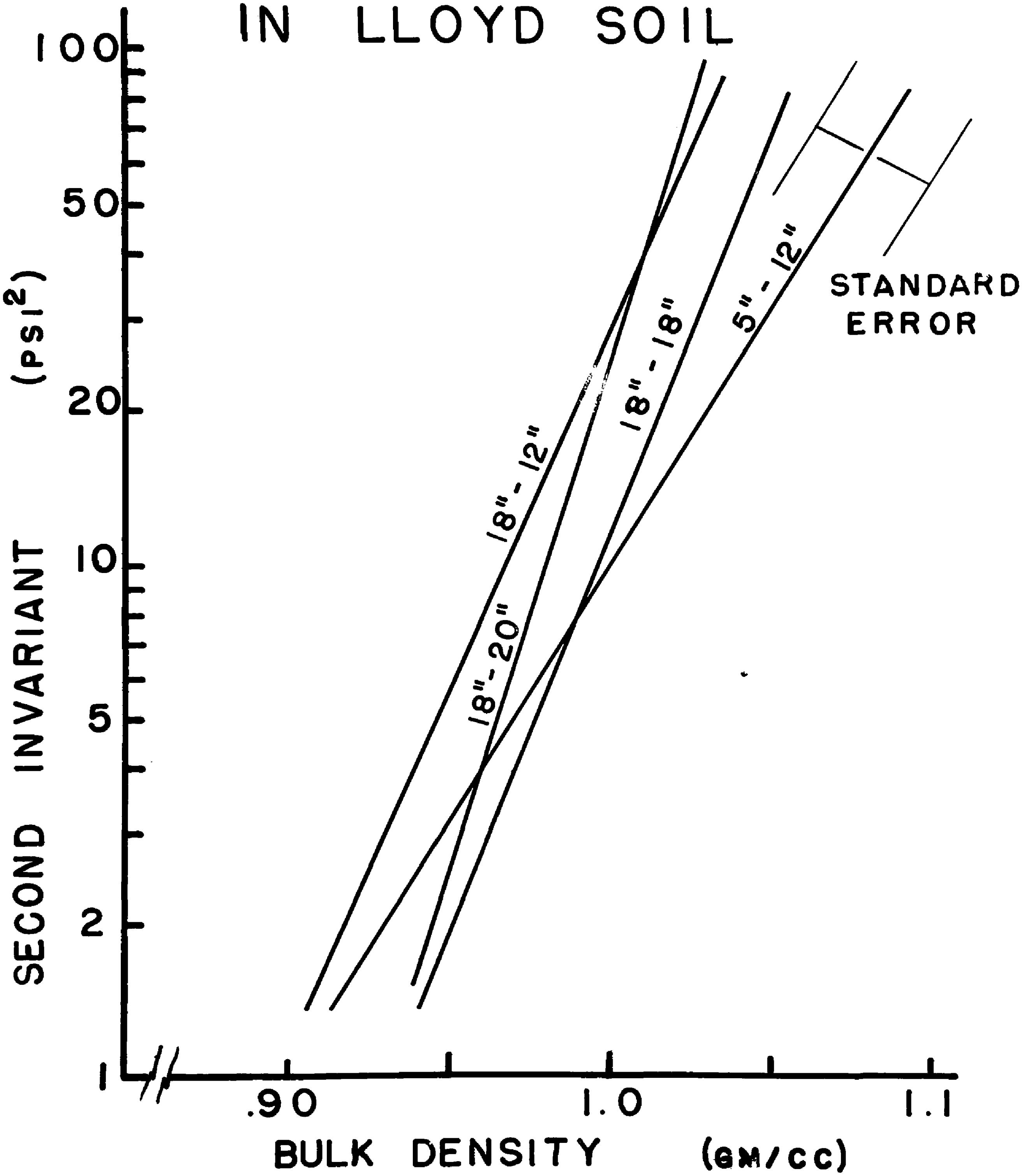

FIG. 24 SECOND INVARIANT OF DEVIATOR VS BULK DENSITY IN DECATUR SOIL

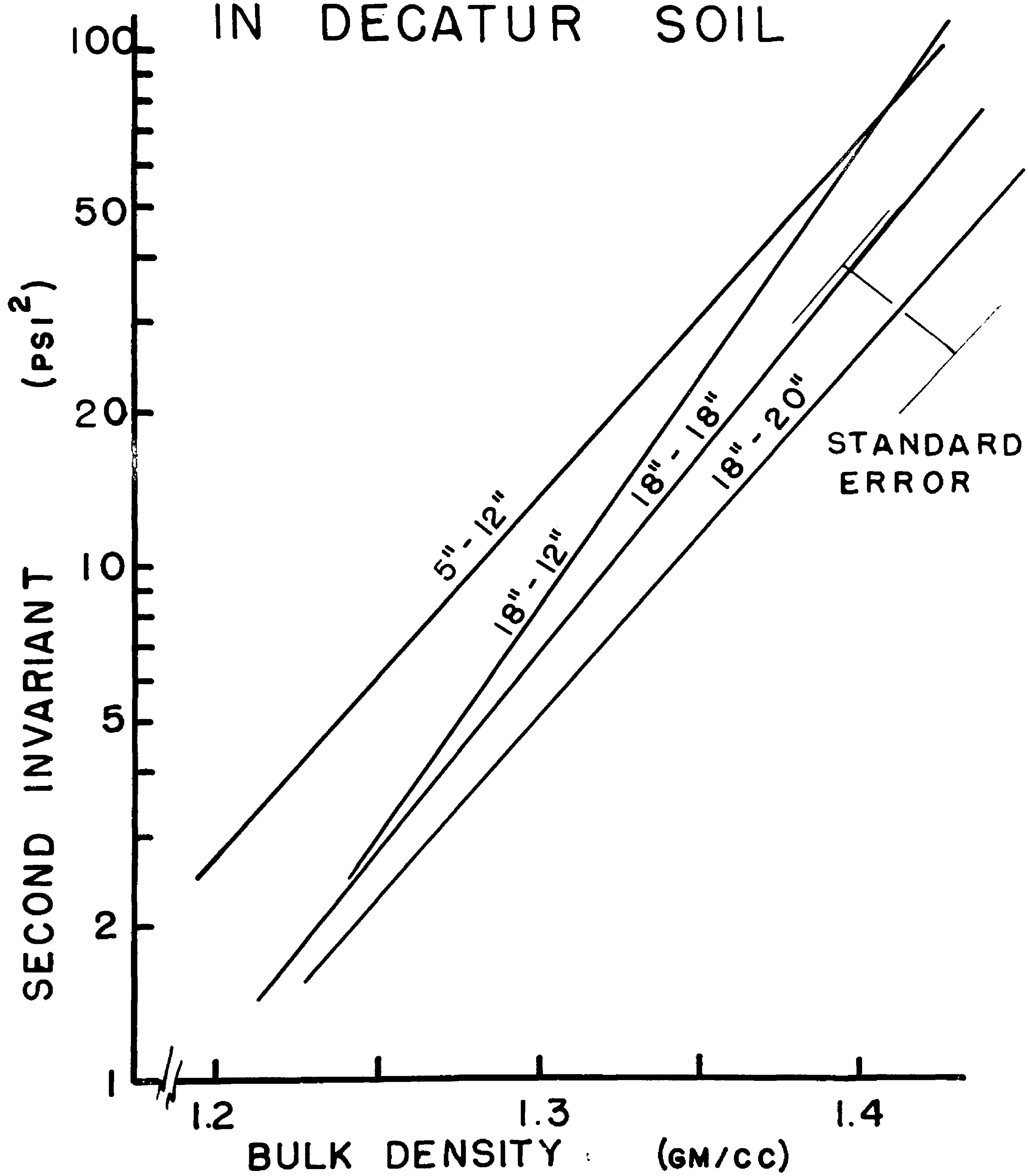

averaged. These values were then used to construct three-dimensional Mohr's circles for each stress state. These circles are shown in Fig. 25 and 26. Note that the representation has the shearing stress plotted against normal stress. The shaded area of the circles represents the possible combinations of normal stress and shearing stress (stress vectors) that can occur on any plane through the point represented. For example, if only a mean normal stress state existed at a point (hydrostatic pressure) Mohr's circles would shrink to a point. If a cylindrical state of stress existed ($\sigma_{II} = \sigma_{III}$) the circles would become one circle with the stress vectors restricted to lie on the circumference of the circle. Figures 25 and 26 clearly indicate that there was very little difference in the four stress states. Consequently, the stress states represent a case of nearly proportional loading. Therefore the lack of significant difference in measures of the deviator does not seem unusual. In spite of the small difference in stress states, the mean normal stress still appears to be the best invariant to relate to bulk density.

The lack of difference in stress states presents some intriguing possibilities. From the Theory of Elasticity, predicted stress distributions under a circular load indicate that the two smaller principal stresses decrease in magnitude faster with depth than the largest principal stress. (Corps of Engineers, 1954.) The ratio of σ_I to an average of σ_{II} and σ_{III} is approximately 3.5 at a location

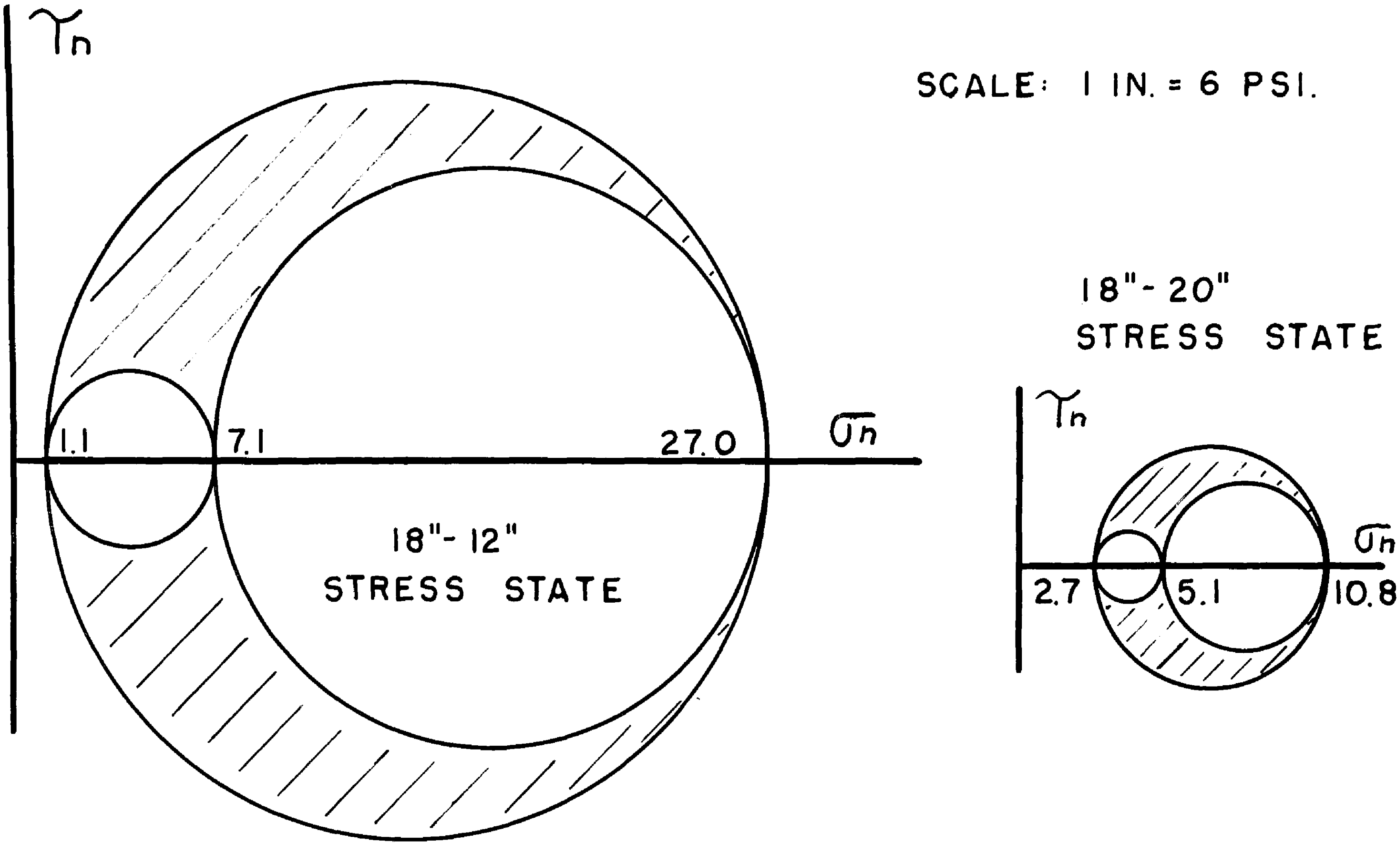

FIG. 25 3 DIMENSIONAL MOHR'S CIRCLES FOR 18"-12" AND 18"-20" STRESS STATES

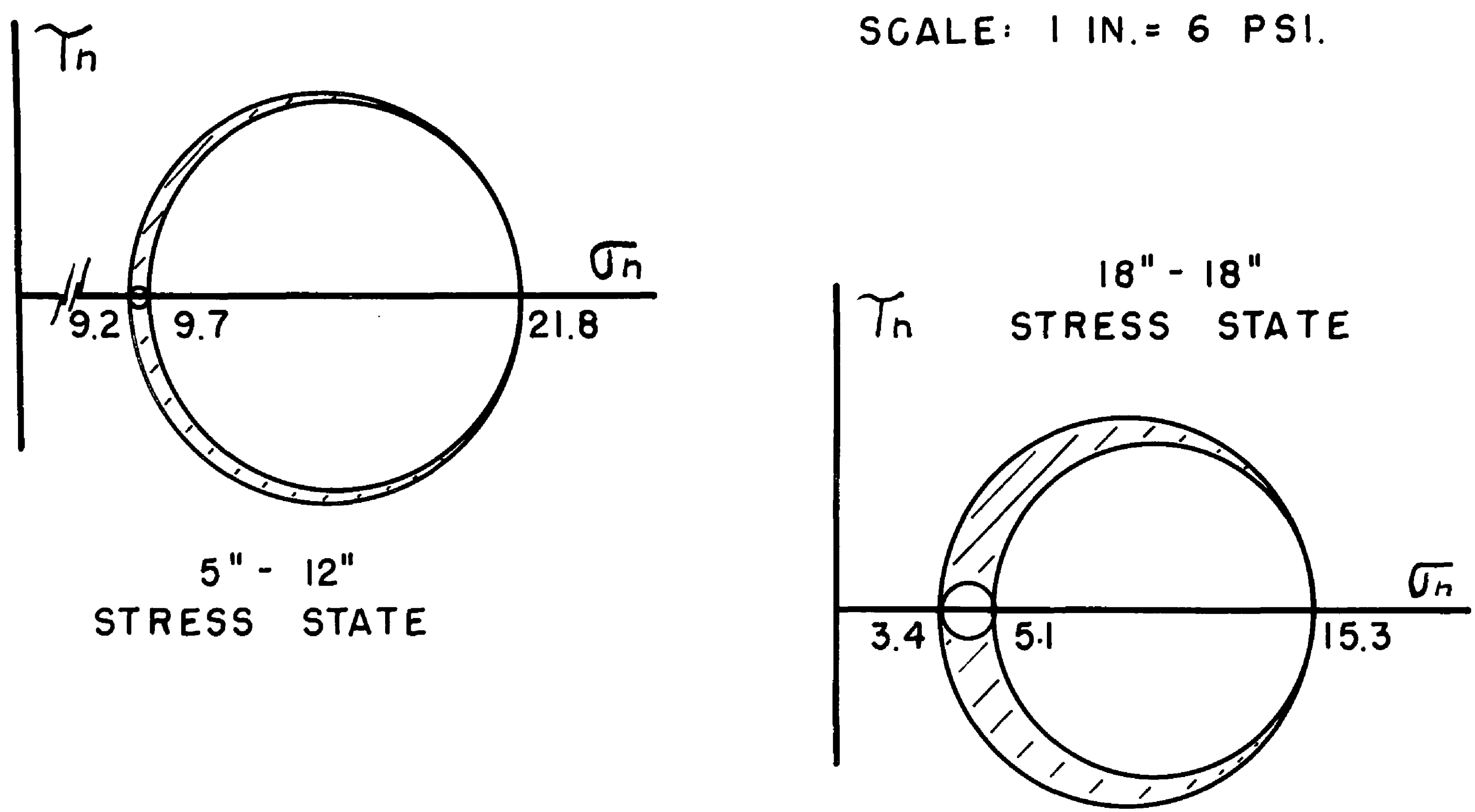

FIG. 26 3 DIMENSIONAL MOHR'S CIRCLES FOR 5"-12" AND 18"-18" STRESS STATES similar to the 5''-12'' stress state in this experiment. For the 5''-12'' stress state, the measured ratio is 2.4. At a location similar to the 18''-20'' stress state, the ratio predicted by Elasticity is approximately 22.6 while the measured ratio is 2.7. At the 18''-12'' stress state Elasticity predicts a ratio of 41.0 while the measured ratio is 6.6. These ratios indicate rather strongly that soil in a loose physical state does not follow an elastic law. It can also be shown that the magnitudes of the measured principal stresses differ greatly from those predicted by Elasticity, particularly at greater depths. It is admitted that the above comparisons are not completely rigorous, but the very large differences lend validity to the conclusions.

Another indication of the similar stress states is the implication of a yield condition for soil. The Coulomb-Mohr formula (equation 14) was discussed as a proposed yield condition for soil. The condition does not specify the plane on which yield occurs but merely states that on some plane the implied relationship exists. If this yield condition is correct, it is possible that when the ratio of the largest principal stress to the smaller principal stresses exceeds a certain value, yield sets in; the soil then relieves itself by deforming such that a new equilibrium is established which does not violate the yield condition. In this manner, the possible stress states the soil can support may be restricted. Assuming the above argument is true, possibly the largest principal stress will always be very nearly proportional to the mean normal stress and, consequently, σ_I can be related to bulk density as well as σ_m. In practice, however, the mean normal stress is much easier to measure than the maximum normal stress. Mean normal stress requires measurement of the normal stress on three mutually perpendicular planes. To measure the maximum normal stress, the entire stress tensor generally needs to be determined and the maximum normal stress then calculated using methods discussed in the preceding section. Thus mean normal stress is preferable.

An indication about the stress distribution under a circular load is shown in Fig. 27. The mean stress for each applied load in a given soil and at a given stress state was averaged. This average was then plotted against the applied load. As can be seen, the distribution of mean normal stress appears to be independent of soil type. The independence implies that the mean normal stress distribution is determined by the geometry of the situation and is independent of soil type. If the above is generally true, it will be possible to determine a stress distribution for a given wheel or implement and the distribution will apply to all soils; the difference in compaction will result from differences in the stress-bulk density relationship for each different soil.

Because of the complex physical nature of soil, there is some question as to the validity of applying continuum mechanics to soil, particularly in a loose condition. The Lloyd clay was a severe test for

FIG. 27 DISTRIBUTION OF MEAN STRESS IN THREE SOILS AND THREE STRESS STATES

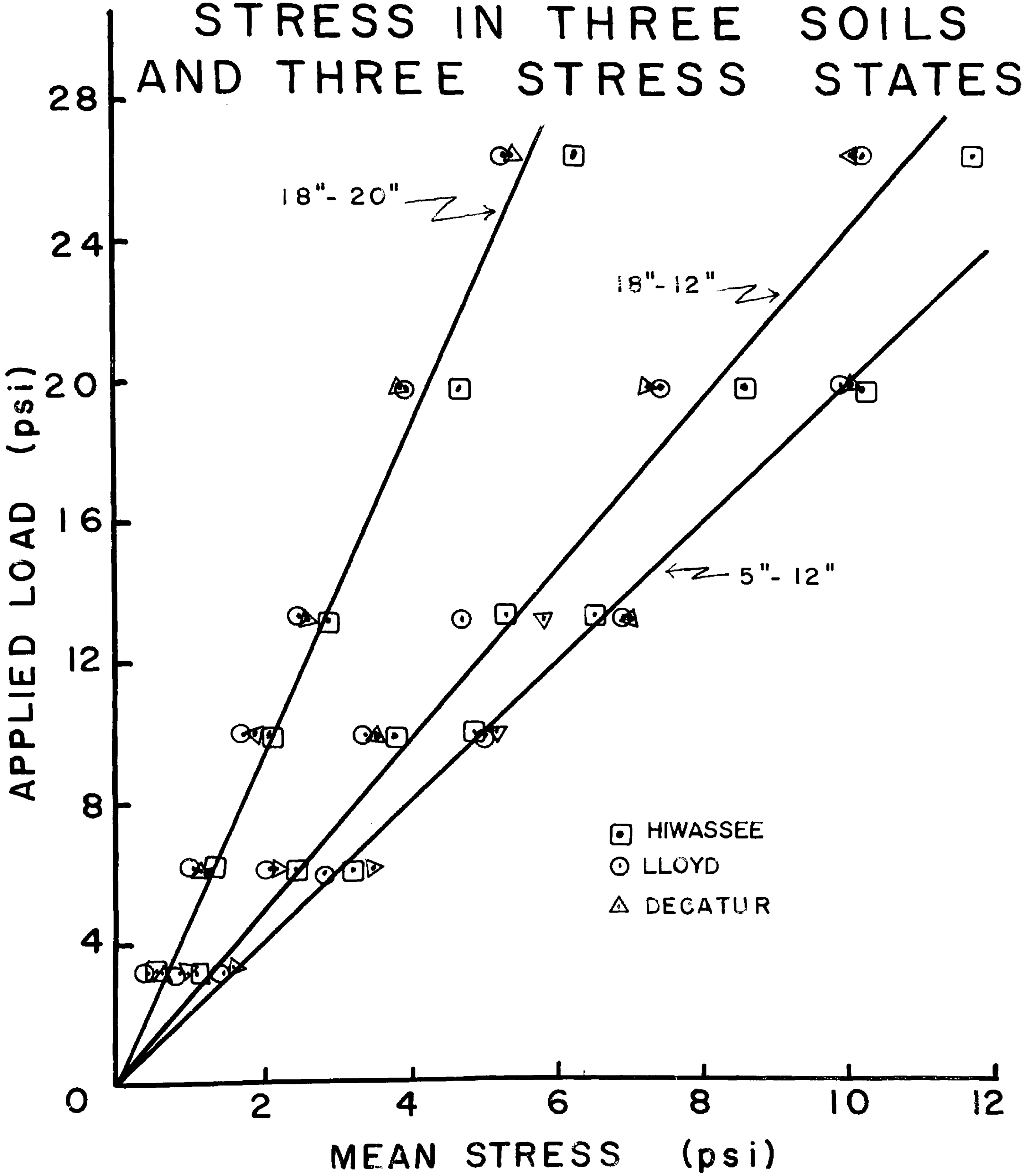

the above question. The soil had been severely compacted, and consequently was lumpy, granular and composed of hard particles. That a good, smooth relationship could be obtained between stress and bulk density readings implies that the concept of the continuum will apply to loose soils. The smooth relationship verifies the statement that the continuum concept is not violated as long as areas large in comparison to the pores and particles actually present in soil are used to make measurements.

LABORATORY TESTS

Procedure.

The basic equipment used in the laboratory tests was the triaxial apparatus manufactured by Soiltest, Inc. model T-108 employing fittings for a 1.4 inch diameter specimen. The apparatus is shown in Fig. 28. The equipment was modified so that air displaced from the soil sample was measured in a U-tube manometer with one side variable, which permitted maintaining atmospheric pressure on the closed system. At the completion of a run, the final volume of the soil sample was determined by weighing mercury displaced by the soil. The best procedure for preparing the sample was found to be transferring the soil by spooning directly into the rubber membrane while in the triaxial apparatus. The membrane itself produced a satisfactory sized specimen and at a lower bulk density than when a mold was used. With this equipment it was possible to apply various stress states to the soil and observe the effect upon the volume change.

In the triaxial apparatus, the force applied to the volume element is controlled. Water pressure applies a mean stress state to the specimen and is one extreme stress state possible with the apparatus. The application of force along the longer axis of the specimen changes the stress state to a so-called cylindrical stress state where the two smaller principal stresses are equal (those applied by water pressure.) Thus the principal stresses are measured directly in the triaxial

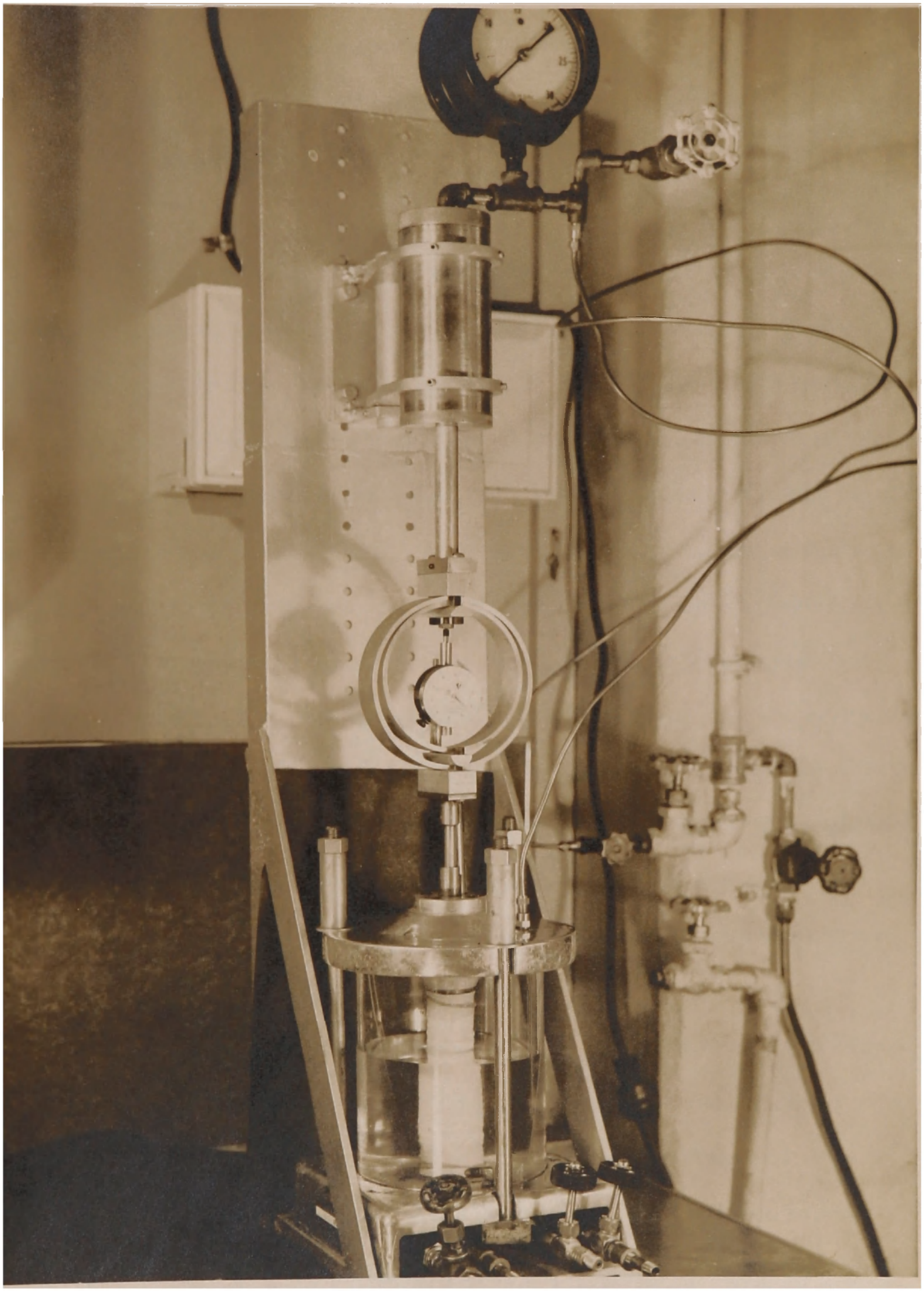

Fig. 28 Triaxial apparatus

apparatus. The other extreme stress state is determined by the magnitude of the largest principal stress before failure of the specimen by shear or overturning.

Results.

The time available at the National Tillage Machinery Laboratory permitted obtaining only a limited amount of data. Most of the data obtained were to test if triaxial apparatus could be used with soils in a very loose condition and to develop techniques for making measurements with such soils. It was determined that triaxial apparatus could be used successfully if proper precautions were taken. One series of tests in the Hiwassee type soil was run where techniques had been developed sufficiently to warrant reporting the data. It should be pointed out, however, that some of the measurements were not as precise as can be obtained. Four individual specimens were tested; two were run with a mean normal stress state applied; two others were run with a cylindrical stress state applied. The results of these four tests are given in Table C. The moisture content of the soil in the laboratory test ran approximately 4% higher than in the field test.

The significance of the tests is the close agreement between laboratory data and field data. The average line for the mean stress-bulk density plot on semi-logarithmic paper and the standard error lines were determined as discussed in Fig. 12. These lines for the triaxial data are shown in Fig. 29. The plotted points are from the

Table C

TRIAXIAL DATA IN
HIWASSEE LOAM SOIL

Spherical stress state		Cylindrical stress state	
Mean Stress (psi)	Bulk Density (gm/cc)	Mean Stress (psi)	Bulk Density (gm/cc)
2.5	1.37	2.5	1.43
5.0	1.53	5.0	1.50
7.5	1.58	10.0	1.58
12.5	1.64	15.0	1.61
20.0	1.70	20.0	1.67
30.0	1.77	30.0	1.71
38.7	1.83	38.7	1.78
2.5	1.43	3.5	1.38
3.9	1.46	6.4	1.51
6.4	1.49	10.4	1.53
7.9	1.54	13.3	1.59
9.3	1.60	20.8	1.61
14.3	1.62	23.7	1.63
17.2	1.66	26.5	1.66
22.2	1.67	36.5	1.68
26.5	1.71		

FIG. 29 FIELD AND TRIAXIAL DATA IN HIWASSEE SANDY LOAM SOIL

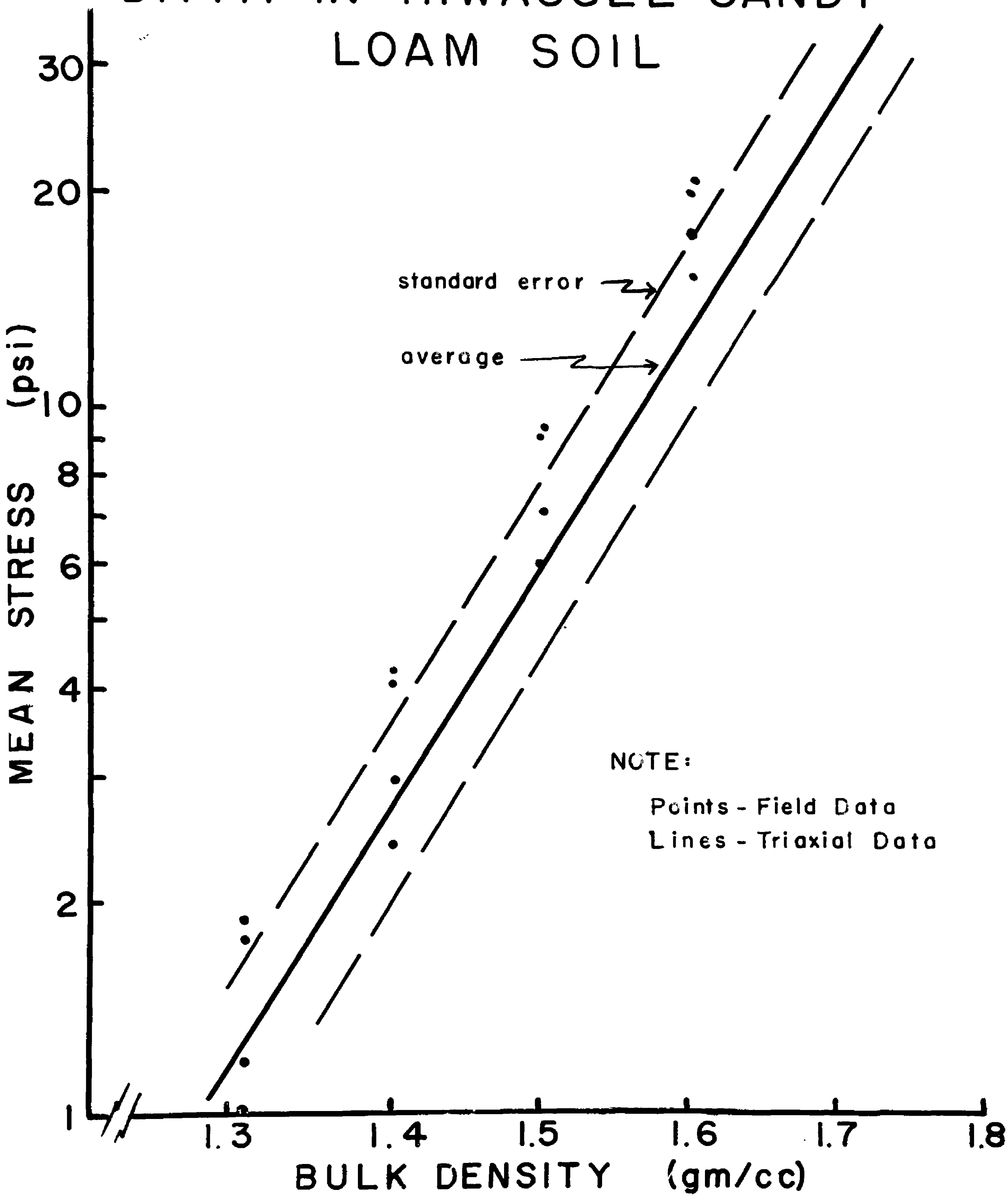

average lines of Fig. 13 of the field data. Since the laboratory soil was at a higher moisture, more compaction should occur for a given loading. (Soehne, 1953; Hovanesian, 1958.) Hence the slight tendency for the field data to be to the left of the average line in Fig. 29 is expected. This good agreement verifies the two methods and lends validity to both techniques for studying the relationship between stress and soil compaction. The success of the laboratory technique provides an effective means for producing different stress states not obtainable under field conditions. Besides the ability to control the stress state accurately, it should be possible to control the variability of the soil somewhat by maintaining uniform soil conditions from test to test. Precise control was not possible in the field tests even with the facilities of the National Tillage Machinery Laboratory, and their long time experience with handling soils.

CONCLUSIONS

In the loose soils tested, the data presented indicate the following;

1.2. Of the four invariants of stress investigated, σ_m , σ_I,

2. Of the four invariants of stress investigated, σ_m , σ_I, $II_{s'}$, τ_{max} , the mean normal stress relates best to bulk density.

3. Because of slight differences in applied stress states and large variation in tests, it cannot be concluded from the tests that soil compaction is independent of the deviator.

4. Triaxial data on the Hiwassee sandy loam soil agreed very closely with field data on the same soil, thus verifying both methods.

5. Triaxial apparatus can be used to study stress-compaction relationships in loose tillable soils and will provide a means of obtaining laboratory control of all variables.

6. The distribution of mean normal stress appears to be independent of soil type and determined only by the geometry of loading.

7. The mean normal stress-bulk density relationship was exponential for all soils tested.

8. Stress distributions predicted by the Theory of Elasticity were not verified in the loose soil used in the experiment.

SUGGESTIONS FOR FURTHER STUDY

1. Verify by additional triaxial tests the hypothesis that mean normal stress is related to soil compaction.

2. Investigate the effect of soil physical properties on the stress-bulk density relationship.

3. Assuming mean normal stress is related to bulk density, calculate, if possible, the mean normal stress distribution under applied loads; if not possible, measure the distribution experimentally.

4. Determine a yield condition for soil which is a function of invariants of the applied stress state.

5. Combining the yield condition and the compaction condition, develop a method for determining the total stress distribution in soil.

6. Determine the difference in above relationships if applied to an undisturbed soil.

7. Apply the above information to tillable soils and calculate magnitude and type of loading to produce a desired state of compaction.

8. Design and test tillage machines or methods which will produce the desired soil physical state.

REFERENCES

Baver, L.D. (1956) Soil Physics, 3rd ed. John Wiley and Sons, Inc., New York.

Cooper, A.W., Glen E. Vanden Berg, H.F. McColly and A.E. Erickson (1957) Strain gage cell measures soil pressure, Agr. Engr.

Corps of Engineers, U.S. Army (1953) Theoretical stresses induced by uniform circular loads, Waterways Expt. Sta., Vicksburg, Miss.

Corps of Engineers, U.S. Army (1954) Homogeneous sand test section, Waterways Expt. Sta., Vicksburg, Miss.

Edminster, T.W. (1956) Progress report of committee on soil compaction, Paper presented at winter meeting of ASAE, Chicago, Ill., Dec. 9-12.

Gill, William R. (1954) Measurement of root growth pressures of seedlings, Agronomy Abstracts. Annual meeting of American Society of Agronomy.

Gill, William R. and Carl A. Reaves (1956) Compaction patterns of smooth rubber tires, Agr. Engr.

Hoffman, O. and G. Sachs (1953) Introduction to the Theory of Plasticity for Engineers, McGraw-Hill Book Co., Inc., New York.

Hogentogler, C.A., (1937) Engineering Properties of Soil, McGraw-Hill Book Co., Inc., New York.

Hovanesian, J.D. (1958) Development and use of a volumetric transducer for studies of parameters upon soil compaction. Thesis for degree of Ph.D., Mich. State Univ., East Lansing, Mich. (Unpublished.)

Jaeger, J.C. (1956) Elasticity, Fracture and Flow, John Wiley and Sons, Inc., New York.

Kelvin, Lord (1902) A New specifying method for stress and strain in an elastic solid, Philosophical Magazine and Journal of Science, Vol. III.

Lee, George Hamor (1950) An Introduction to Experimental Stress Analysis, John Wiley and Sons, Inc., New York.

Malvern, L.E. (1956) Introduction to the mechanics of a continuous medium, Unpublished notes for graduate course in Applied Mechanics Dept., Mich. State Univ.

McKibben, Eugene and Robert L. Green (1940) Relative effects of steel wheels and pneumatic tires on agricultural soils, Agr. Engr.

Peattie, K. R. and R. W. Sparrow (1954) The Fundamental action of earth pressure cells, Journal of the Mechanics and Physics of Solids, Vol. 2.

Plummer, Fred L. and Stanley M. Dore (1940) Soil Mechanics and Foundations, Pitman Publishing Corp., New York.

Reed, I. F. (1940) A Method of studying soil packing by tractors, Agr. Engr.

Russell , E. W. and W. Belcerek (1944) The Determination of the volume and air space of soil clods, Journal of Agri. Sci. 34:123-132.

Soehne, Walter (1953) Druckverteilung in Boden und Bodenverformung unter Schlepperreifen (Distribution of pressure in the soil and soil deformation under tractor tires) Grdlhn D. Landtechn, 5:49-63.

Timoshenko, S. and J. N. Goodier (1951) Theory of Elasticity, McGraw-Hill Book Co., Inc., 2nd ed., New York.

Torstensson, G. and S. Erickson (1936) A New method for determining the porosity of the soil, Soil Sci. 42: 406-416.

Vanden Berg, G.E., A.W. Cooper, A.E. Erickson, W.M. Carleton (1957) Soil pressure distribution under tractor and implement traffic, Agr. Engr.

Veihmeyer, F. J. (1929) An Improved soil sampling tube, Soil Sci. 27: 147-152.

Wadleigh, C. H. (1957) Growth of plants. Soil: The Yearbook of Agriculture 1957. The U.S. Govt. Printing Ofc, Washington,D.C.

Wiersma, D. and M. M. Mortland (1953) Response of sugar beets to peroxide fertilization and its relation to oxygen diffusion. Soil Sci. 75: 355-360.

Willits, Nathan A. (1956) Measurement of pressures in soils produced by traffic and the relationship between those pressures and compaction in undisturbed soils, Unpublished Ph.D. thesis presented to Michigan State Univ.

APPENDIX

TABLE I HIWASSEE SANDY LOAM 5"-12"

Load (psi)	Bulk Density (gm/cc)	σ_x (psi)	σ_y (psi)	σ_z (psi)	σ_n (psi)	σ_I (psi)	σ_{II} (psi)	σ_{III} (psi)	τ_{max} (psi)	σ_m (psi)	$II_{s'}$ (psi^2)	ϕ Deg.
Rep.2												
3.3	1.35	1.2	0.7	2.4	1.7	2.4	1.2	0.7	0.8	1.4	0.8	5.6
6.2	1.42	2.3	1.1	4.7	3.4	4.8	2.3	1.0	1.9	2.7	3.7	7.7
9.9	1.46	3.5	2.1	7.4	5.4	7.5	3.5	2.0	2.7	4.3	7.9	6.8
13.3	1.49	4.6	3.2	10.0	7.4	10.1	4.6	3.1	3.5	5.9	13.5	6.3
19.8	1.52	7.1	6.4	15.5	11.9	15.6	7.1	6.3	4.7	9.7	26.6	5.8
26.5	1.56	9.8	9.6	20.9	17.0	21.1	9.8	9.3	5.9	13.4	45.0	8.4
Rep.3												
3.3	1.24	1.2	0.7	3.8	2.0	3.8	1.2	0.7	1.6	1.9	2.9	-5.0
6.2	1.33	2.3	1.8	7.1	4.0	7.1	2.3	1.7	2.7	3.7	8.7	-4.8
9.9	1.40	3.5	2.8	10.0	6.3	10.0	3.5	2.8	3.6	5.4	15.8	-1.3
13.3	1.44	4.6	3.9	13.0	8.2	13.0	4.6	3.9	4.6	7.2	25.6	-1.2
19.8	1.50	7.0	6.9	18.3	12.8	18.3	6.9	6.9	5.7	10.7	43.3	1.0
26.5	1.54	9.3	9.9	22.7	17.0	22.7	9.8	9.3	6.7	14.0	57.9	3.1
Rep.4												
3.3	1.26	1.2	1.1	3.0	1.7	3.0	1.2	1.0	1.0	1.7	1.3	-8.9
6.2	1.35	2.3	2.1	5.7	3.4	5.7	2.3	2.1	1.8	3.4	4.2	-7.4
9.9	1.42	3.5	2.8	8.6	5.1	8.7	3.5	-2.8	3.0	5.0	10.5	-5.9
13.3	1.47	4.6	4.2	11.6	6.8	11.8	4.6	4.1	3.8	6.8	18.3	-8.1
19.8	1.52	7.3	6.7	17.3	10.2	17.6	7.3	6.4	5.6	10.4	38.5	-9.4
26.5	1.58	10.0	9.2	22.0	14.2	22.2	10.0	9.0	6.6	13.7	53.4	-6.0
Rep.5												
3.3	1.24	1.2	0.7	2.7	1.7	2.7	1.2	0.7	1.0	1.5	1.0	0.4
6.2	1.33	2.3	1.8	5.3	3.4	5.3	2.3	1.8	1.8	3.1	5.6	-2.0
9.9	1.38	3.5	2.8	8.3	5.7	8.3	3.5	2.8	2.7	4.8	8.8	1.4
13.3	1.43	4.4	3.5	11.2	7.7	11.2	4.4	3.5	3.8	6.4	17.6	2.2
19.8	1.48	6.8	6.4	16.5	11.9	16.5	6.8	6.4	5.1	9.9	[illegible]	2.1
26.5	1.54	9.3	9.2	21.2	13.5	21.3	9.3	9.1	6.1	13.2	49.5	6.0

TABLE II HIWASSEE SANDY LOAM 18"-12"

Load (psi)	Bulk Density (gm/cc)	σ_x (psi)	σ_y (psi)	σ_z (psi)	σ_h (psi)	σ_I (psi)	σ_{II} (psi)	σ_{III} (psi)	τ_{max} (psi)	σ_m (psi)	$II_{s'}$ (psi^2)	ϕ Deg.
Rep 1												
3.3	1.21	0.6	0.6	2.0	1.5	2.0	0.6	0.6	0.7	1.1	0.7	8.1
6.2	1.28	1.5	1.4	4.8	4.0	5.0	1.5	1.2	1.9	2.6	4.6	13.4
9.9	1.36	2.1	2.4	7.6	6.4	8.0	2.1	2.0	3.0	4.1	11.6	13.8
13.3	1.39	3.1	3.5	10.4	9.2	11.1	3.1	2.8	4.1	5.7	22.0	16.8
19.8	1.47	5.4	6.4	15.5	15.8	17.6	5.4	4.3	6.7	9.1	54.8	24.0
26.5	1.49	9.6	9.8	20.0	23.6	25.0	9.6	4.9	10.0	13.1	110.1	29.8
Rep 2												
3.3	1.31	0.6	0.5	2.8	1.7	2.8	0.6	0.5	1.2	1.3	1.7	0.0
6.2	1.38	1.3	1.0	6.4	4.2	6.4	1.3	1.0	2.7	2.9	9.6	3.4
9.9	1.43	1.9	1.8	9.6	6.6	9.7	1.9	1.7	4.0	4.4	21.1	6.3
13.3	1.47	2.3	2.3	12.0	8.8	12.3	2.3	2.0	5.2	5.5	34.4	9.1
19.8	1.54	4.2	4.3	20.0	16.5	21.1	4.2	3.1	9.0	9.5	102.2	14.5
26.5	1.60	5.6	6.0	25.4	22.7	27.6	5.6	3.8	11.9	12.3	175.8	17.8
Rep 3												
3.3	1.23	0.3	0.5	1.6	1.7	1.9	0.3	0.2	0.8	0.8	0.8	24.7
6.2	1.30	0.8	1.1	4.0	4.2	4.7	0.8	0.4	2.2	2.0	5.7	24.0
9.9	1.36	1.2	1.9	6.4	7.2	7.9	1.2	0.4	3.8	3.2	17.0	27.0
13.3	1.39	2.0	2.6	9.2	10.6	11.6	2.0	0.2	5.7	4.6	37.8	27.5
19.8	1.45	3.8	4.5	14.4	17.2	18.6	3.8	0.3	9.2	7.6	95.2	28.6
26.5	1.49	5.0	6.3	17.9	22.9	24.4	5.0	-0.2	12.3	9.7	167.4	30.8
Rep 4												
3.3	1.21	0.4	0.3	1.6	2.0	2.2	0.4	-0.3	1.3	0.8	1.7	26.8
6.2	1.29	1.3	0.9	4.0	5.0	5.4	1.3	-0.5	3.0	2.0	9.2	28.9
9.9	1.35	2.1	1.4	6.8	8.3	9.1	2.1	-0.9	5.0	3.4	26.0	28.5
13.3	1.37	3.3	2.1	9.6	12.5	13.5	3.3	-1.7	7.6	5.0	80.1	30.0
19.8	1.42	5.7	3.1	14.8	20.9	22.2	5.7	-4.3	13.3	7.9	170.9	32.0
26.5	1.46	10.6	4.8	20.0	29.0	30.1	10.6	-5.9	18.3	11.8	335.1	32.7
Rep 5												
3.3	1.29	0.4	0.4	2.4	2.0	2.6	0.4	0.2	1.2	1.0	1.7	15.0
6.2	1.37	1.0	1.0	5.6	4.6	6.0	1.0	0.7	2.7	2.6	8.8	14.9
9.9	1.43	1.7	1.8	9.2	7.3	9.6	1.7	1.4	4.1	4.2	21.9	12.6
13.3	1.45	2.3	2.6	12.0	10.3	12.9	2.3	1.8	5.6	5.6	39.5	16.0
19.8	1.57	3.5	4.9	18.2	17.5	20.5	3.5	2.6	8.9	6.9	101.1	21.0
26.5	1.59	4.8	7.4	23.2	25.1	27.9	4.8	2.7	12.6	11.8	195.2	25.6

TABLE III HIWASSEE SANDY LOAM 18"-18"

Load (psi)	Bulk Density (gm/cc)	σ_x (psi)	σ_y (psi)	σ_z (psi)	σ_n (psi)	σ_I (psi)	σ_{II} (psi)	σ_{III} (psi)	τ_{max} (psi)	σ_m (psi)	$II_{s'}$ (psi^2)	ϕ Deg.
Rep 1												
3.3	1.23	0.0	0.4	1.2	1.3	1.5	0.1	0.0	0.7	0.5	0.7	26.5
6.2	1.30	0.4	1.0	3.2	2.6	3.6	0.9	0.4	1.4	1.5	2.4	13.0
9.9	1.36	0.8	1.5	5.2	4.0	5.3	1.4	0.8	2.2	2.5	5.9	9.0
13.3	1.38	1.2	2.3	7.2	5.3	7.3	2.2	1.2	3.0	3.6	10.5	6.1
19.8	1.43	1.9	3.8	11.6	8.1	11.6	3.7	1.9	4.9	5.7	26.8	3.3
26.5	1.47	2.8	5.4	15.4	10.9	16.4	6.4	2.8	6.8	6.5	49.7	-2.8
Rep 2												
3.3	1.30	0.4	0.5	1.6	1.5	1.6	0.4	0.4	0.6	0.8	0.5	13.2
6.2	1.38	0.8	1.1	2.8	2.6	5.0	0.9	0.8	1.1	1.6	1.6	19.4
9.9	1.43	1.0	1.9	4.4	4.0	4.6	1.6	1.0	1.8	2.4	3.7	16.5
13.3	1.46	1.7	2.8	5.6	5.3	6.0	2.4	1.7	2.2	3.3	5.3	12.7
19.8	1.49	2.7	5.0	8.8	8.2	9.2	4.6	2.7	3.3	5.5	11.3	17.5
26.5	1.52	4.2	8.5	12.0	11.2	12.2	8.3	4.2	4.0	8.2	16.3	14.4
Rep 3												
3.3	1.26	0.2	0.4	2.1	1.5	2.2	0.3	0.2	1.0	0.9	1.2	6.7
6.2	1.35	0.4	0.9	4.3	3.0	4.3	0.8	0.4	2.0	1.9	4.6	8.0
9.9	1.42	0.8	1.5	6.1	4.6	6.3	1.4	0.8	2.7	2.8	9.0	9.4
13.3	1.45	1.2	2.1	8.0	6.4	8.3	1.8	1.2	3.5	3.8	15.2	11.9
19.8	1.49	2.3	3.4	11.7	9.9	12.3	2.8	2.3	5.0	5.8	32.0	14.7
26.5	1.53	3.7	4.8	15.0	13.9	16.4	3.7	3.5	6.4	7.9	54.3	18.8
Rep 4												
3.3	1.31	0.4	0.4	1.1	1.1	1.2	0.4	0.2	0.5	0.6	0.3	24.0
6.2	1.40	0.6	0.9	2.4	2.6	2.9	0.6	0.4	1.2	1.3	1.9	23.5
9.9	1.44	1.0	1.5	3.7	4.0	4.4	1.0	0.9	1.7	2.1	3.9	25.2
13.3	1.45	1.5	2.3	5.6	5.7	6.3	1.5	1.3	2.5	3.0	7.9	25.3
19.8	1.48	2.3	3.8	7.8	9.2	9.8	2.3	1.7	4.0	4.6	20.1	30.0
26.5	1.56	3.3	6.0	10.7	13.6	14.0	3.3	2.6	5.7	6.7	41.3	33.0
Rep 5												
3.3	1.27	0.4	0.5	1.9	1.3	1.9	0.5	0.4	0.7	0.9	0.7	5.5
6.2	1.34	0.8	1.3	4.0	3.1	4.1	1.2	0.8	1.6	2.0	3.2	5.7
9.9	1.40	1.0	2.0	5.9	4.8	6.1	1.8	1.0	2.5	3.0	7.3	12.5
13.3	1.44	1.5	2.8	7.7	7.0	8.3	2.2	1.5	3.4	4.0	14.3	17.8
19.8	1.54	2.5	4.5	11.2	11.4	12.7	3.0	2.5	5.1	6.1	33.3	23.4
26.5	1.56	3.8	7.0	14.4	13.7	17.7	3.8	3.7	7.0	8.4	35.6	29.0

TABLE IV HIWASSEE SANDY LOAM 18"-20"

Load (psi)	Bulk Density (gm/cc)	σ_x (psi)	σ_y (psi)	σ_z (psi)	σ_n (psi)	σ_I (psi)	σ_{II} (psi)	σ_{III} (psi)	τ_{max} (psi)	σ_m (psi)	$II_{s'}$ (psi^2)	ϕ Deg.
Rep 1												
3.3	1.24	0.4	0.7	1.0	1.3	1.3	0.4	0.4	0.5	0.7	0.3	34.5
6.2	1.31	1.0	1.4	2.2	3.0	3.0	1.0	0.6	1.2	1.5	1.8	35.7
9.9	1.36	1.5	2.1	3.4	4.8	4.9	1.5	0.6	2.2	2.4	5.2	36.8
13.3	1.39	1.9	2.8	4.5	6.5	6.6	1.9	0.7	3.0	3.1	10.0	37.5
19.8	1.45	2.7	5.0	6.8	9.7	9.8	2.7	2.0	3.9	4.9	18.5	38.2
26.5	1.48	3.5	6.7	8.7	13.4	13.5	3.5	1.9	5.8	6.5	39.3	41.7
Rep 2												
3.3	1.27	0.4	0.4	1.0	0.6	1.0	0.4	0.3	0.4	0.6	0.2	-9.6
6.2	1.34	0.8	1.4	2.4	1.8	2.4	1.4	0.8	0.8	1.5	0.6	-2.4
9.9	1.39	1.2	2.1	3.8	3.0	3.8	2.1	1.2	1.3	2.4	1.8	0.7
13.3	1.42	1.2	2.8	4.6	3.7	4.6	2.8	1.2	1.7	2.8	2.9	-0.3
19.8	1.47	1.9	5.4	8.0	6.7	8.0	5.4	1.9	3.0	5.1	9.2	-0.8
26.5	1.52	2.4	7.8	10.2	8.8	10.2	7.8	2.4	3.9	6.8	15.8	-4.3
Rep 3												
3.3	1.21	0.2	0.4	1.0	1.4	1.5	0.2	-0.1	0.8	0.5	0.7	22.5
6.2	1.27	0.4	1.1	2.2	3.0	3.1	0.4	0.2	1.5	1.2	2.7	23.5
9.9	1.33	0.8	1.8	3.4	4.3	4.4	0.8	0.7	1.9	2.0	4.6	22.0
13.3	1.34	1.0	2.5	4.6	7.7	7.8	1.0	-0.8	4.3	2.7	20.5	28.0
19.8	1.39	1.7	4.2	7.1	10.1	10.3	1.7	1.0	4.6	4.4	26.8	26.0
26.5	1.43	2.4	5.7	8.8	11.2	11.5	3.0	2.4	4.5	5.3	25.9	23.8
Rep 4												
3.3	1.24	0.0	0.4	1.2	1.6	1.7	0.0	-0.1	0.9	0.5	1.0	21.4
6.2	1.31	0.4	0.7	2.2	2.6	2.8	0.4	0.1	1.3	1.1	2.2	28.0
9.9	1.35	0.6	1.8	3.2	3.7	3.9	1.1	0.6	1.7	1.9	3.2	29.0
13.3	1.38	1.0	2.8	4.3	5.0	5.1	2.0	1.0	2.1	2.7	4.8	21.5
19.8	1.43	1.9	4.6	6.3	7.4	7.6	3.7	1.9	2.8	4.3	8.6	21.7
26.5	1.45	2.9	7.8	8.8	9.9	10.0	6.6	2.9	3.6	6.5	12.7	26.0
Rep 5												
3.3	1.26	0.4	0.0	1.2	1.0	1.3	0.4	-0.1	0.7	0.5	0.5	17.0
6.2	1.30	0.3	0.7	2.2	2.0	2.4	0.6	0.5	0.9	1.2	1.1	17.5
9.9	1.38	1.0	1.4	3.4	3.0	3.6	1.2	1.0	1.3	1.9	2.0	15.1
13.3	1.41	1.5	2.1	4.6	3.8	4.7	2.0	1.5	1.6	2.7	2.8	10.3
19.8	1.49	2.5	4.2	6.6	5.7	6.7	4.2	2.5	2.1	4.5	4.4	5.3
26.5	1.50	3.7	5.0	9.0	7.4	9.0	4.9	3.7	2.7	5.9	7.9	5.5

TABLE V LLOYD CLAY 5"-12"

Load (psi)	Bulk Density (gm/cc)	σ_x (psi)	σ_y (psi)	σ_z (psi)	σ_n (psi)	σ_I (psi)	σ_{II} (psi)	σ_{III} (psi)	τ_{max} (psi)	σ_m (psi)	$II_{s'}$ (psi^2)	ϕ Deg.
Rep 1												
3.3	0.93	0.9	0.4	3.0	1.7	3.0	0.9	0.3	1.3	1.4	1.9	1.1
6.2	0.96	1.9	1.1	5.9	2.8	6.0	1.9	1.0	2.5	3.0	7.1	-7.2
9.9	1.00	3.1	2.1	8.8	4.2	9.1	3.1	1.9	3.6	4.7	14.9	-10.3
13.3	1.03	4.1	3.0	11.8	5.7	12.1	4.1	2.6	4.7	6.3	26.0	-10.3
19.8	1.06	6.2	5.4	17.1	8.5	17.7	6.2	4.8	6.5	9.5	50,3	-12.5
26.5	1.10	8.1	8.1	21.2	11.4	22.0	8.1	7.4	7.3	12.5	67.7	-13.3
Rep 2												
3.3	0.94	1.2	0.4	3.0	1.7	3.0	1.2	0.3	1.3	1.5	1.8	1.1
6.2	0.98	2.3	1.4	6.6	3.6	6.6	2.3	1.4	2.6	3.4	7.8	-4.0
9.9	1.00	3.5	2.8	10.2	5.4	10.4	3.5	2.7	3.8	5.5	17.8	-7.7
13.3	1.02	4.8	3.9	13.6	7.4	13.8	4.8	3.7	5.0	7.4	30.8	-7.3
19.8	1.08	7.2	6.4	19.5	11.4	19.7	7.2	6.2	6.7	11.0	56.3	-6.4
26.5	1.10	9.4	8.5	23.8	15.2	23.8	9.4	8.4	7.7	13.9	74.5	-3.0
Rep 3												
3.3	0.89	1.2	1.0	2.7	1.1	2.9	1.2	0.7	1.1	1.6	1.3	-19.5
6.2	0.95	2.3	2.0	5.3	2.3	5.8	2.3	1.5	2.2	3.2	5.2	-19.7
9.9	0.99	3.6	2.8	8.1	3.4	8.8	3.6	2.1	3.4	4.9	12.5	-18.6
13.3	1.04	5.0	3.8	11.5	5.1	12.3	5.0	3.0	4.6	6.8	23.6	-16.6
19.8	1.06	7.3	5.7	16.0	7.9	16.7	7.3	4.9	5.9	9.6	39.3	-14.5
26.5	1.10	9.3	7.8	20.4	11.4	20.9	9.3	7.2	6.8	12.5	54.8	-11.5
Rep 4												
3.3	0.93	1.1	0.7	2.7	1.4	2.8	1.1	0.6	1.1	1.5	1.5	-9.4
6.2	0.97	2.3	1.4	5.9	2.8	6.0	2.3	1.3	2.4	3.2	6.3	-10.0
9.9	0.99	3.5	2.1	9.1	4.3	9.4	3.5	1.9	3.8	4.9	15.8	-10.6
13.3	1.01	4.6	3.2	12.2	5.8	12.6	4.6	2.8	4.9	6.7	26.8	-11.2
19.8	1.05	6.8	5.3	17.4	9.0	17.8	6.8	4.8	6.5	9.6	49.1	-10.7
26.5	1.10	8.9	7.6	21.6	11.9	22.3	8.9	7.0	7.7	12.7	69.6	-10.6
Rep 5												
3.3	0.97	1.2	0.7	2.9	1.5	3.0	1.2	0.7	1.2	1.6	1.5	-8.6
6.2	1.00	2.2	1.4	6.2	3.2	6.3	2.2	1.4	2.4	3.3	6.9	-6.5
9.9	1.03	3.3	2.3	9.4	5.1	9.5	3.3	2.2	3.6	5.0	15.4	-6.3
13.3	1.06	4.6	3.1	13.0	7.4	13.0	4.6	3.1	5.0	6.9	28.8	-3.9
19.8	1.10	6.6	4.7	18.3	11.2	18.3	6.6	4.7	6.8	9.8	54.6	-1.[illegible]
26.5	1.11	8.9	6.4	22.4	14.8	22.4	8.9	6.4	8.0	12.5	74.5	-1.3

TABLE VI LLOYD CLAY 18"-12"

Load (psi)	Bulk Density (gm/cc)	σ_x (psi)	σ_y (psi)	σ_z (psi)	σ_n (psi)	σ_I (psi)	σ_{II} (psi)	σ_{III} (psi)	τ_{max} (psi)	σ_m (psi)	$II_{s'}$ (psi^2)	ϕ Deg.
Rep 1												
3.3	0.90	0.4	0.3	2.0	1.3	2.0	0.4	0.3	0.8	0.9	0.9	5.2
6.2	0.91	1.0	0.8	4.5	3.2	4.5	1.0	0.8	1.9	2.1	4.5	7.6
9.9	0.93	1.5	1.5	7.2	5.5	7.4	1.5	1.3	3.1	3.4	12.2	11.2
13.3	0.94	2.2	2.3	9.8	8.3	10.4	2.2	1.7	4.4	4.8	23.8	15.5
19.8	0.98	3.7	4.4	15.1	14.4	16.8	3.7	2.6	7.1	7.7	62.8	20.6
26.5	1.02	5.4	6.7	19.9	21.0	23.4	5.4	3.2	10.1	10.7	123.2	24.7
Rep 2												
3.3	0.94	0.0	0.5	1.8	1.5	1.9	0.4	0.0	0.9	0.8	1.0	15.6
6.2	0.95	0.6	1.2	4.0	4.0	4.6	0.6	0.6	2.0	1.9	5.2	22.2
9.9	0.98	1.2	2.0	6.2	6.6	7.4	1.2	0.8	3.3	3.2	13.5	24.7
13.3	1.01	2.3	2.9	8.6	9.9	10.8	2.3	0.6	5.1	4.6	29.6	28.0
19.8	1.06	3.5	4.9	13.4	17.3	18.3	3.5	-0.1	9.2	7.3	95.2	31.3
26.5	1.08	5.1	7.1	17.6	24.2	25.3	5.1	-0.6	14.9	8.9	134.9	35.2
Rep 5												
3.3	0.94	0.4	0.8	1.6	1.0	1.6	0.7	0.4	0.6	0.9	0.4	-13.8
6.2	0.96	1.0	1.5	4.0	2.6	4.0	1.5	1.0	1.5	2.2	2.6	- 2.7
9.9	0.98	1.5	2.3	6.4	4.8	6.5	2.3	1.5	2.5	3.4	7.2	6.4
13.3	1.02	2.1	3.1	8.8	7.4	9.1	2.8	2.1	3.5	4.7	15.1	13.2
19.8	1.05	3.5	5.1	14.0	13.9	15.8	3.5	3.4	6.2	7.5	50.7	22.0
26.5	1.06	5.0	7.0	18.7	20.1	22.2	5.0	3.6	9.3	10.2	107.0	25.5
Rep 6												
3.3	0.93	0.4	0.4	1.6	1.3	1.7	0.4	0.3	0.7	0.8	0.6	14.2
6.2	0.95	1.2	0.9	4.0	3.3	4.2	1.2	0.6	1.8	2.0	3.6	14.5
9.9	0.98	2.1	1.4	6.2	5.5	6.8	2.1	0.9	2.9	3.2	9.5	16.9
13.3	1.00	2.9	2.0	8.6	8.4	9.8	2.9	0.7	4.6	4.5	22.6	22.0
19.8	1.04	4.9	3.5	12.8	14.5	16.1	4.9	0.0	8.0	7.0	67.9	26.7
26.5	1.06	6.7	4.3	17.1	21.1	22.9	6.7	-1.5	12.2	9.3	155.0	29.0
Rep 1	18"-20"											
3.3	0.90	0.2	0.0	1.3	1.2	1.5	0.2	-0.2	0.8	0.5	0.8	19.0
6.2	0.92	0.3	0.6	2.7	2.4	2.9	0.3	0.3	1.3	1.2	2.2	18.0
9.9	0.94	0.6	1.3	3.8	3.6	4.2	0.9	0.6	1.8	1.9	3.9	19.0
13.3	0.95	0.8	1.8	5.2	4.8	5.7	1.4	0.8	2.4	2.6	7.1	18.9
19.8	0.96	1.3	3.2	7.5	7.1	8.1	2.6	1.3	3.4	4.0	13.2	19.3
26.5	0.99	2.0	4.8	9.4	9.2	10.2	4.0	2.0	4.1	5.4	18.3	20.6

TABLE VII LLOYD CLAY 18"-18"

Load (psi)	Bulk Density (gm/cc)	σ_x (psi)	σ_y (psi)	σ_z (psi)	σ_n (psi)	σ_I (psi)	σ_{II} (psi)	σ_{III} (psi)	τ_{max} (psi)	σ_m (psi)	II_s' (psi^2)	ϕ Deg.
Rep 1	0.97	0.3	0.4	1.6	1.3	1.7	0.3	0.3	0.7	0.8	0.6	14.4
3.3	0.97	0.3	0.4	1.6	1.3	1.7	0.3	0.3	0.7	0.8	0.6	14.4
6.2	0.97	0.7	0.8	3.7	2.9	3.7	0.7	0.7	1.6	1.7	3.3	10.6
9.9	0.97	1.0	1.5	5.6	4.4	5.8	1.3	1.0	2.4	2.7	7.1	11.3
13.3	0.99	1.5	2.2	7.5	6.2	7.8	1.9	1.5	3.2	3.7	12.6	13.2
19.8	1.02	2.5	3.8	11.6	10.0	12.2	3.1	2.5	4.8	6.0	29.5	15.0
26.5	1.05	3.3	5.3	16.0	14.3	17.1	4.1	3.3	6.9	8.2	60.0	17.0
Rep 2												
3.3	0.93	0.2	0.2	1.1	0.9	1.1	0.2	0.2	0.4	0.5	0.5	14.2
6.2	0.94	0.6	0.7	2.3	2.2	2.6	0.6	0.4	1.1	1.2	1.4	20.5
9.9	0.95	1.0	1.1	3.7	3.1	3.9	1.0	1.0	1.4	2.0	2.8	13.0
13.3	0.96	1.5	1.7	4.8	4.8	5.5	1.5	1.0	2.2	2.6	6.1	23.0
19.8	1.01	2.2	3.0	7.5	7.7	8.5	2.2	1.9	3.3	4.2	14.0	25.8
26.5	1.04	3.2	4.5	9.7	10.8	11.6	3.2	2.6	4.5	5.5	25.3	27.5
Rep 3												
3.3	0.91	0.3	0.4	2.1	1.3	2.1	0.4	0.3	0.9	1.0	1.1	1.7
6.2	0.94	0.6	0.8	4.4	2.8	4.4	0.7	0.6	1.9	1.9	4.6	3.2
9.9	0.96	0.8	1.2	6.7	4.6	6.8	1.2	0.8	3.0	2.9	11.1	6.7
13.3	1.00	1.2	1.8	8.8	6.7	9.0	1.5	1.2	3.9	3.9	19.4	10.4
19.8	1.02	1.7	2.9	12.6	10.6	13.4	2.1	1.7	5.8	5.7	44.0	15.2
26.5	1.04	2.5	4.0	16.3	15.4	18.2	2.5	2.1	8.1	7.6	84.7	20.2
Rep 4												
3.3	0.95	0.0	0.2	1.1	1.3	1.4	0.0	-0.1	0.8	0.4	0.7	26.0
6.2	0.95	0.4	0.8	2.7	2.8	3.2	0.4	0.2	1.5	1.3	2.7	24.5
9.9	0.97	0.8	1.3	3.7	4.6	4.9	0.8	0.1	2.4	1.9	6.8	29.7
13.3	0.98	1.0	2.0	5.1	6.6	7.0	1.0	0.2	3.4	2.7	13.7	31.5
19.8	1.02	1.7	3.1	7.5	10.9	11.3	1.7	-0.7	6.0	4.1	40.6	39.4
26.5	1.04	2.5	4.4	9.3	15.2	15.6	2.5	-1.8	8.7	5.4	81.9	36.8
Rep 5												
3.3	0.94	0.4	0.5	1.6	1.3	1.7	0.4	0.4	0.6	0.8	0.5	13.0
6.2	0.97	0.8	1.0	2.7	2.6	2.9	0.8	0.7	1.1	1.5	1.5	20.3
9.9	0.99	1.2	1.6	4.1	3.8	4.4	1.3	1.2	1.6	2.3	3.4	19.5
13.3	1.03	1.7	2.6	5.3	5.5	6.0	1.9	1.7	2.2	3.2	6.1	24.0
19.8	1.06	2.5	4.1	7.0	8.0	8.3	2.8	2.5	2.9	4.5	10.7	29.8
26.5	1.07	3.8	5.9	8.5	10.3	10.6	3.9	3.8	3.4	6.1	15.2	33.5

TABLE VIII LLOYD CLAY 18"-20"

Load (psi)	Bulk Density (gm/cc)	σ_x (psi)	σ_y (psi)	σ_z (psi)	σ_n (psi)	σ_I (psi)	σ_{II} (psi)	σ_{III} (psi)	τ_{max} (psi)	σ_m (psi)	$II_{s'}$ (psi^2)	ϕ Deg
Rep 2												
3.3	0.91	0.2	0.2	1.0	1.4	1.5	0.2	-0.3	0.9	0.5	0.9	32.8
6.2	0.93	0.5	0.8	2.1	3.1	3.2	0.5	-0.3	1.8	1.1	3.5	35.0
9.9	0.94	0.7	1.7	3.0	4.9	5.0	0.7	-0.3	2.6	1.8	8.0	38.2
13.3	0.96	0.9	2.6	4.1	6.8	6.9	0.9	-0.3	3.6	2.5	14.8	39.0
19.8	0.99	1.5	4.5	6.0	9.9	9.9	1.5	0.5	4.7	4.1	26.7	40.2
26.5	1.00	2.3	6.6	7.6	12.3	12.3	2.3	1.8	5.2	5.5	35.1	42.8
Rep 3												
3.3	0.90	0.0	0.0	0.7	0.6	0.8	0.0	-0.1	0.4	0.2	0.2	14.2
6.2	0.90	0.3	0.4	2.1	1.7	2.2	0.3	0.2	1.0	0.9	1.3	13.8
9.9	0.92	0.7	0.8	2.8	3.0	3.3	0.7	0.3	1.5	1.4	2.7	25.0
13.3	0.94	1.1	1.6	3.8	4.5	4.8	1.1	0.6	2.1	2.2	5.4	28.7
19.8	0.96	1.8	3.0	5.8	7.1	7.4	1.8	1.3	3.1	3.5	11.5	31.5
26.5	0.97	2.7	4.5	7.5	9.7	10.0	2.7	2.0	4.0	4.9	19.4	33.8
Rep 4												
3.3	0.93	0.2	0.3	1.0	0.9	1.1	0.2	0.2	0.5	0.5	0.3	18.5
6.2	0.94	0.5	0.8	2.2	2.2	2.4	0.6	0.5	1.0	1.2	1.2	21.2
9.9	0.96	0.8	1.4	3.2	3.4	3.7	0.9	0.8	1.5	1.8	2.8	25.0
13.3	0.97	1.2	2.1	4.4	4.7	5.1	1.4	1.2	2.0	2.6	4.9	25.7
19.8	1.01	1.9	3.9	7.3	7.7	8.3	2.9	1.9	3.2	4.4	11.7	25.3
26.5	1.04	2.7	5.7	8.7	9.9	10.3	4.1	2.7	3.8	5.7	16.3	30.4
Rep 5												
3.3	0.92	0.2	0.0	0.8	1.2	1.3	0.2	-0.5	0.9	0.3	0.8	31.6
6.2	0.93	0.4	0.3	1.8	2.8	3.0	0.4	-0.9	2.0	0.8	4.0	33.8
9.9	0.95	0.6	0.6	2.8	4.7	4.8	0.6	-1.5	3.2	1.3	10.5	35.0
13.3	0.97	0.8	1.1	3.8	6.4	6.6	0.8	-1.7	4.2	1.9	18.2	36.0
19.8	0.99	1.5	2.1	5.6	9.7	9.9	1.5	-2.2	6.0	3.1	38.5	36.8
26.5	1.03	2.0	3.2	7.2	12.2	12.5	2.0	-2.1	7.3	4.1	56.5	37.4
Rep 6												
3.3	0.93	0.6	0.6	0.9	1.0	1.0	0.6	0.4	0.3	0.7	0.1	29.9
6.2	0.95	1.2	1.1	2.0	2.1	2.2	1.2	0.9	0.7	1.4	0.5	26.2
9.9	0.98	1.5	1.8	3.0	3.2	3.4	1.5	1.4	1.0	2.1	1.3	28.4
13.3	0.99	2.3	2.8	4.0	4.5	4.7	2.3	2.1	1.3	3.0	2.0	31.3
19.8	1.02	3.5	4.6	5.8	7.1	7.2	3.5	3.2	2.0	4.6	4.9	36.0
26.5	1.06	4.6	6.4	7.6	9.1	9.2	4.8	4.6	2.3	6.2	6.7	37.3

TABLE IX DECATUR SILTY CLAY LOAM 5"-12"

Load (psi)	Bulk Density (gm/cc)	σ_x (psi)	σ_y (psi)	σ_z (psi)	σ_n (psi)	σ_I (psi)	σ_{II} (psi)	σ_{III} (psi)	τ_{max} (psi)	σ_m (psi)	II_{s}' (psi^2)	ϕ Deg.
Rep 1												
3.3	1.15	1.2	0.8	2.4	1.7	2.4	1.2	0.8	0.8	1.4	0.7	3.5
6.2	1.22	2.3	1.4	5.6	4.0	5.6	2.3	1.3	2.2	3.1	5.1	6.6
9.9	1.28	3.5	2.2	9.1	5.7	9.1	3.5	2.2	3.4	4.9	13.4	0.4
13.3	1.31	4.6	3.4	12.1	7.9	12.1	4.6	3.4	4.4	6.7	22.3	0.9
19.8	1.36	6.6	5.4	17.7	11.6	17.7	6.6	5.4	6.2	9.9	46.0	0.5
26.5	1.41	8.9	8.0	22.1	15.3	22.1	8.9	8.0	7.0	13.0	62.4	1.0
Rep 2												
3.3	1.17	1.6	1.4	2.4	1.7	2.4	1.6	1.4	0.5	1.8	0.3	-10.8
6.2	1.24	2.3	2.1	5.0	3.4	5.0	2.3	2.1	1.4	3.1	2.6	-2.9
9.9	1.28	3.5	3.2	7.7	5.1	7.7	3.5	3.2	2.3	4.8	6.5	-4.3
13.3	1.30	4.6	4.2	10.6	6.8	10.6	4.6	4.1	3.2	6.5	13.2	-5.3
19.8	1.33	6.8	6.4	15.6	10.2	15.7	6.8	6.3	4.7	9.6	27.7	-4.9
26.5	1.38	8.9	8.8	20.1	13.6	20.2	8.9	8.7	5.7	12.6	42.9	-4.3
Rep 3												
3.3	1.12	0.8	0.7	3.2	1.7	3.2	0.8	0.7	1.3	1.6	2.1	-5.6
6.2	1.21	1.9	1.4	6.2	3.4	6.2	1.9	1.4	2.4	3.2	7.1	-4.2
9.9	1.28	3.1	2.8	10.6	6.2	10.6	3.1	2.8	3.9	5.5	19.8	-5.6
13.3	1.32	4.2	3.5	13.6	8.2	13.6	4.2	3.5	5.1	7.1	31.9	-1.9
19.8	1.36	6.2	5.3	18.9	11.9	18.9	6.2	5.3	6.8	10.1	57.9	-0.9
26.5	1.38	8.1	7.1	23.0	15.9	23.0	8.1	7.0	8.0	12.7	80.0	-3.0
Rep 4												
3.3	1.19	1.2	0.7	2.4	1.4	2.4	1.2	0.7	0.9	1.4	0.8	-3.3
6.2	1.26	2.3	1.8	4.7	3.1	4.7	2.3	1.8	1.5	2.9	2.4	-2.9
9.9	1.31	4.1	3.5	8.8	5.7	8.8	4.1	3.5	2.7	5.5	8.6	-4.8
13.3	1.35	5.0	4.2	11.8	7.4	11.8	5.0	4.2	3.8	7.0	17.8	-4.4
19.8	1.38	7.7	6.4	16.5	10.8	16.5	7.7	6.4	5.1	10.2	30.6	-3.7
26.5	1.43	9.8	8.5	20.6	13.9	20.6	9.8	8.5	6.1	13.0	44.5	-3.0

TABLE X DECATUR SILTY CLAY LOAM 18"-12"

Load (psi)	Bulk Density (gm/cc)	σ_x (psi)	σ_y (psi)	σ_z (psi)	σ_n (psi)	σ_I (psi)	σ_{II} (psi)	σ_{III} (psi)	τ_{max} (psi)	σ_m (psi)	Π_s' (psi^2)	ϕ Deg.
Rep 1												
3.3	1.15	0.4	0.2	1.6	1.3	1.7	0.4	0.1	0.8	0.7	0.7	14.8
6.2	1.22	0.8	1.0	4.0	3.3	4.2	0.8	0.8	1.7	1.9	3.9	15.1
9.9	1.26	1.5	1.8	6.4	5.6	6.8	1.5	1.4	2.7	3.2	9.8	16.5
13.3	1.32	2.1	2.9	8.8	8.2	9.6	2.1	2.1	3.8	4.6	18.9	19.3
19.8	1.38	3.7	4.8	13.6	13.9	15.6	3.7	2.8	6.4	7.4	51.5	23.5
26.5	1.48	5.4	7.0	18.0	20.5	22.2	5.4	2.8	9.7	10.1	111.1	27.8
Rep 2												
3.3	1.14	0.4	0.4	1.6	1.3	1.7	0.4	0.3	0.7	0.8	0.6	13.2
6.2	1.21	1.2	1.0	4.8	3.3	4.8	1.2	1.0	1.9	2.3	4.7	5.8
9.9	1.31	2.1	1.6	7.2	5.6	7.4	2.1	1.4	3.0	3.6	11.0	11.6
13.3	1.33	2.9	2.2	10.0	8.2	10.5	2.9	1.7	4.4	5.0	25.0	14.2
19.8	1.38	4.6	4.0	15.2	14.5	17.0	4.6	2.2	7.4	7.9	63.7	20.6
26.5	1.43	6.7	6.1	20.0	21.4	23.9	6.7	2.2	10.9	10.9	131.5	25.3
Rep 3												
3.3	1.21	0.4	0.5	1.6	1.3	1.7	0.4	0.4	0.6	0.8	0.5	12.2
6.2	1.27	1.0	1.0	3.6	3.3	3.9	1.0	0.7	1.6	1.9	3.3	18.7
9.9	1.30	1.9	1.9	6.0	5.3	6.4	1.9	1.5	2.4	3.3	7.4	16.6
13.3	1.35	2.7	2.6	8.0	8.2	9.3	2.7	1.3	4.0	4.4	18.0	23.6
19.8	1.38	4.4	4.4	12.0	14.5	16.6	4.4	0.8	7.4	6.9	58.9	29.5
26.5	1.42	6.2	6.5	16.0	21.1	22.2	6.2	0.3	10.9	9.6	128.1	32.0
Rep 4												
3.3	1.22	0.4	0.6	2.4	2.0	2.5	0.5	0.4	1.1	1.1	1.5	14.5
6.2	1.28	0.8	1.2	4.0	5.0	5.4	0.8	-0.2	2.8	2.0	8.8	25.0
9.9	1.38	1.7	2.2	8.0	9.6	10.4	1.7	-0.2	5.3	4.0	32.5	28.7
13.3	1.40	2.5	3.0	10.0	13.2	14.1	2.5	-1.0	7.6	5.2	62.5	31.2
19.8	1.44	4.2	4.5	13.6	20.1	21.0	4.2	-2.9	12.0	7.4	150.6	33.7
26.5	1.50	5.8	6.5	17.6	27.4	28.4	5.8	-4.3	16.3	10.0	279.4	35.0
Rep 5												
3.3	1.21	0.4	0.5	2.0	1.3	2.0	0.5	0.4	0.8	1.0	0.8	1.9
6.2	1.28	1.0	1.2	4.4	4.6	5.2	1.0	0.4	2.4	2.2	6.9	24.0
9.9	1.31	1.7	2.1	6.8	7.8	8.5	1.7	0.4	4.1	3.5	19.3	27.5
13.3	1.38	2.5	3.3	8.8	11.2	11.8	2.5	0.2	5.8	4.9	37.7	21.6
19.8	1.44	4.2	5.0	12.8	16.5	19.3	4.2	-1.5	10.4	7.3	114.7	34.0
26.5	1.48	5.8	7.3	16.8	22.9	23.9	5.8	0.2	11.8	10.0	153.3	35.1

TABLE XI DECATUR SILTY CLAY LOAM 18"-18"

Load (psi)	Bulk Density (gm/cc)	σ_x (psi)	σ_y (psi)	σ_z (psi)	σ_n (psi)	σ_I (psi)	σ_{II} (psi)	σ_{III} (psi)	τ_{max} (psi)	σ_m (psi)	$II_{s'}$ (psi^2)	ϕ Deg.
Rep 1												
3.3	1.26	0.0	0.2	1.3	1.3	1.5	0.0	-0.1	0.8	0.5	0.8	22.5
6.2	1.32	0.4	0.8	3.2	3.1	3.6	0.4	0.4	1.6	1.5	3.5	21.3
9.9	1.36	0.8	1.2	5.5	5.3	6.2	0.8	0.4	2.9	2.5	10.6	21.2
13.3	1.41	1.2	1.9	6.9	7.5	8.4	1.2	0.4	4.0	3.3	19.3	25.5
19.8	1.47	2.1	3.3	9.9	11.9	12.8	2.1	0.4	6.2	5.1	45.7	29.0
26.5	1.52	2.9	4.6	12.8	16.7	17.7	2.9	-0.3	9.0	6.8	92.0	31.7
Rep 2												
3.3	1.18	0.2	0.2	1.1	0.7	1.1	0.2	0.2	0.4	0.5	0.3	3.2
6.2	1.25	0.6	0.8	2.1	2.9	3.0	0.6	-0.1	1.6	1.2	2.8	33.0
9.9	1.29	1.0	1.2	3.5	4.6	4.9	1.0	-0.2	2.5	1.9	7.0	31.5
13.3	1.31	1.4	1.8	4.8	6.6	6.9	1.4	-0.3	3.6	2.7	14.3	33.8
19.8	1.38	2.3	3.0	6.9	10.6	10.9	2.3	-1.0	6.0	4.1	38.1	25.6
26.5	1.47	2.9	4.3	8.8	15.0	15.3	2.9	-2.2	8.7	5.3	80.9	37.6
Rep 3												
3.3	1.18	0.2	0.2	3.2	1.5	3.2	0.2	0.2	1.5	1.2	3.0	- 3.8
6.2	1.25	0.4	0.8	5.6	3.5	5.6	0.8	0.4	2.6	2.3	8.5	3.5
9.9	1.32	1.2	1.8	9.6	6.6	9.7	1.7	1.2	4.2	4.2	22.8	6.9
13.3	1.38	1.7	2.5	11.7	8.8	12.0	2.2	1.7	5.2	5.3	33.8	10.0
19.8	1.43	2.3	4.0	15.8	13.6	16.9	2.9	2.3	7.3	7.4	67.8	16.0
26.5	1.46	3.3	5.8	19.0	18.9	21.7	3.3	3.1	9.3	9.4	114.0	13.2
Rep 4												
3.3	1.20	0.4	0.2	1.6	1.3	1.7	0.4	0.1	0.8	0.7	0.7	14.8
6.2	1.25	0.8	0.8	3.2	3.1	3.6	0.8	0.4	1.6	1.6	3.1	21.1
9.9	1.30	1.2	1.5	5.6	5.5	6.4	1.2	0.7	2.8	2.8	9.8	21.9
13.3	1.34	1.7	2.2	7.5	8.1	9.0	1.7	0.6	4.2	3.8	20.9	25.4
19.8	1.37	2.5	3.8	10.7	12.8	13.8	2.5	0.7	6.5	5.7	50.2	29.2
26.5	1.40	3.3	5.8	13.9	18.0	19.0	3.3	0.7	9.1	7.7	97.1	32.0

TABLE XII DECATUR SILTY CLAY LOAM 18"-20"

Load (psi)	Bulk Density (gm/cc)	σ_x (psi)	σ_y (psi)	σ_z (psi)	σ_n (psi)	σ_I (psi)	σ_{II} (psi)	σ_{III} (psi)	τ_{max} (psi)	σ_m (psi)	$II_{s'}$ (psi^2)	ϕ Deg.
Rep 1												
3.3	1.16	0.4	0.4	0.9	1.1	1.2	0.4	0.2	0.5	0.6	0.3	30.5
6.2	1.21	0.8	0.7	1.9	2.3	2.5	0.8	0.1	1.2	1.1	1.4	29.5
9.9	1.25	1.2	1.5	3.0	3.4	3.6	1.2	0.9	1.4	1.9	2.3	28.5
13.3	1.31	1.9	2.4	3.7	4.5	4.6	1.9	1.5	1.6	2.7	3.0	33.0
19.8	1.33	3.1	3.9	5.3	6.5	6.6	3.1	2.6	2.0	4.1	4.9	35.0
26.5	1.39	4.6	5.7	6.6	8.8	8.8	4.6	3.5	2.7	5.6	8.0	40.2
Rep 2												
3.3	1.14	0.2	0.4	1.2	1.1	1.3	0.3	0.2	0.6	0.6	0.4	18.3
6.2	1.20	0.4	0.7	2.6	2.3	2.8	0.5	0.4	1.2	1.2	1.8	17.1
9.9	1.28	0.8	1.4	3.8	3.6	4.2	1.0	0.8	1.6	2.0	3.5	19.7
13.3	1.28	1.2	1.8	5.3	4.8	5.7	1.4	1.2	2.2	2.8	6.5	17.7
19.8	1.34	1.9	2.8	7.8	7.2	8.4	2.2	1.9	3.3	4.2	13.7	18.5
26.5	1.38	3.1	4.2	10.2	9.6	11.0	3.4	3.1	4.0	5.8	20.4	19.3
Rep 3												
3.3	1.20	0.4	0.0	0.9	1.4	1.5	0.4	-0.6	1.0	0.4	1.1	32.4
6.2	1.24	0.8	0.7	1.6	3.1	3.2	0.8	-0.8	2.0	1.0	4.0	38.5
9.9	1.27	1.2	1.1	3.0	4.5	4.8	1.2	-0.6	2.6	1.8	7.8	34.5
13.3	1.30	1.5	1.4	3.8	6.0	6.2	1.5	-1.0	3.6	2.2	13.4	35.5
19.8	1.33	2.2	2.8	5.6	8.8	9.0	2.2	-0.6	4.8	3.5	24.5	36.7
26.5	1.37	3.1	4.2	7.4	11.1	11.3	3.1	0.3	5.5	4.9	33.1	36.8
Rep 4												
3.3	1.25	0.0	0.3	1.3	1.4	1.6	0.0	0.0	0.8	0.5	0.8	25.2
6.2	1.32	0.4	0.6	2.4	3.1	3.3	0.4	-0.3	1.8	1.1	3.8	30.4
9.9	1.37	0.8	1.1	3.8	5.4	5.7	0.8	-0.8	3.2	1.9	11.4	32.6
13.3	1.39	1.0	1.3	5.0	7.1	7.5	1.0	-1.2	4.4	2.4	20.6	32.5
19.8	1.44	1.5	2.0	6.8	9.9	10.4	1.5	-1.6	6.0	3.4	38.8	33.3
26.5	1.46	2.3	3.0	8.6	12.4	13.0	2.3	-1.4	7.2	4.6	55.5	33.6
Rep 5												
3.3	1.18	0.2	0.0	0.9	1.1	1.2	0.2	-0.3	0.8	0.4	0.6	27.8
6.2	1.24	0.4	0.7	2.1	2.6	2.8	0.4	0.0	1.4	1.1	2.3	30.0
9.9	1.28	0.8	1.4	3.2	4.0	4.2	0.8	0.4	1.9	1.6	4.5	31.0
13.3	1.32	1.2	2.1	4.6	5.7	6.0	1.2	0.7	2.7	2.6	8.6	31.0
19.8	1.37	1.5	3.5	6.9	8.8	9.2	1.5	1.2	4.0	4.0	20.4	32.2
26.5	1.41	2.3	5.7	9.1	11.9	12.2	2.6	2.3	5.0	5.7	31.6	34.7